

LA-UR-99-2318

C.3

**THE LOS ALAMOS NATIONAL LABORATORY ATMOSPHERIC  
TRANSPORT AND DIFFUSION MODELS:  
USERS MANUAL**

by

M. Williams, T. Yamada, S. Bunker, and E. Niccum

March 1989



SCANNED

APR 4 1999



## CONTENTS

I. INTRODUCTION . . . . .	1
II. OPERATIONAL PROCEDURE . . . . .	1
III. DESCRIPTION OF MODELS . . . . .	27
IV. FINITE-DIFFERENCE EQUATIONS AND A GRID SYSTEM . . . . .	42
ACKNOWLEDGEMENTS . . . . .	51

## I. INTRODUCTION

The LANL atmospheric transport and diffusion models are composed of two state-of-the-art computer codes. The first is an atmospheric wind model called HOTMAC, Higher Orders Turbulence Model for Atmospheric Circulations. HOTMAC generates wind and turbulence fields by solving a set of atmospheric dynamic equations. The second is an atmospheric diffusion model called RAPTAD, RANdom Particle Transport And Diffusion. RAPTAD uses the wind and turbulence output from HOTMAC to compute particle trajectories and concentration at any location downwind from a source. Both of these models, originally developed as research codes on supercomputers, have been modified to run on microcomputers. Because the capability of microcomputers is advancing so rapidly, the expectation is that they will eventually become as good as today's supercomputers.

Now both models are run on desktop or desktop computers, such as an IBM PC/AT with an Opus Pm 350-32 bit coprocessor board and a SUN workstation. Codes have also been modified so that high level graphics, NCAR Graphics, of the output from both models are displayed on the desktop computer monitors and plotted on a laser printer. Two programs, HOTPLT and RAPLOT, produce wind vector plots of the output from HOTMAC and particle trajectory plots of the output from RAPTAD, respectively. A third CONPLT provides concentration contour plots.

Section II describes step-by-step operational procedures, specifically for a SUN-4 desktop computer, on how to run main programs HOTMAC and RAPTAD, and graphics programs to display the results. Governing equations, boundary conditions and initial values of HOTMAC and RAPTAD are discussed in Section III. Finite-difference representations of the governing equations, numerical solution procedures, and a grid system are given in Section IV.

## II. OPERATIONAL PROCEDURE

Figure 1 shows how the various programs work together in six steps, which are described in detail below.

### **STEP 1: Set Up Input for HOTMAC**

Setting up input for HOTMAC is accomplished in two steps. The first step (1a)

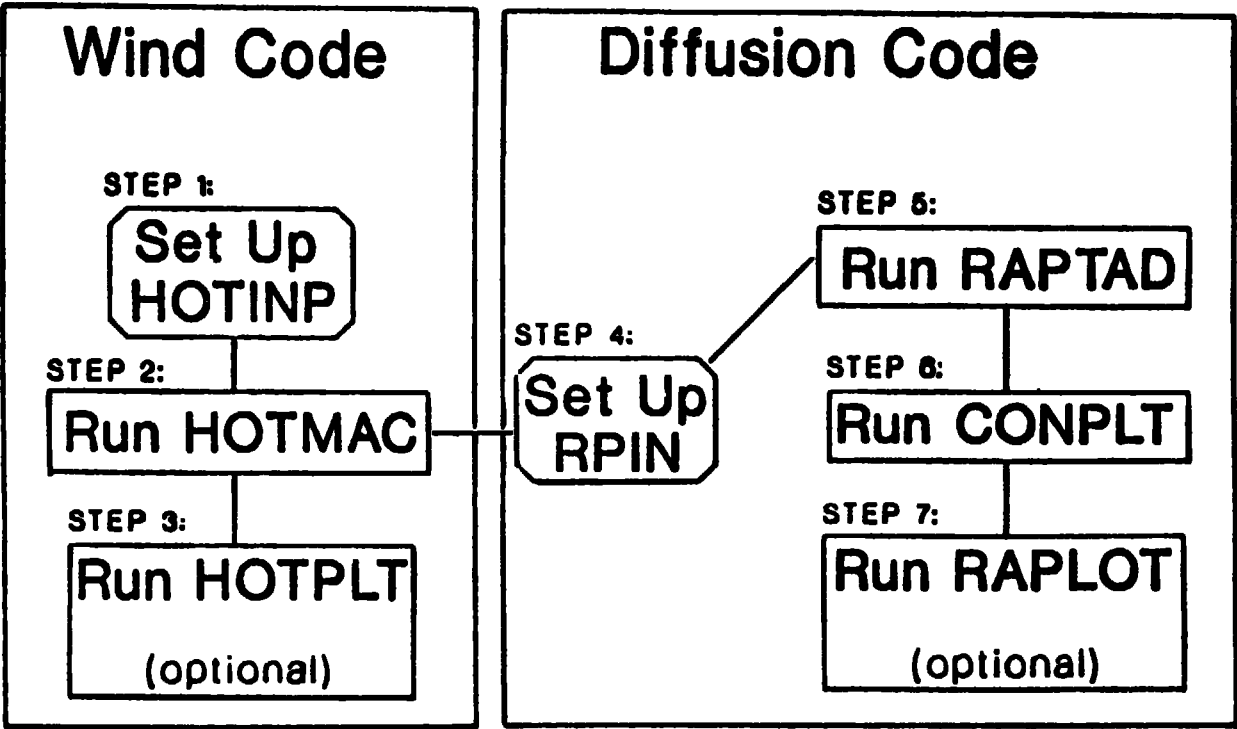


**Fig. 1.** Schematic diagram of the major steps and computer codes used in the present system.

involves modifying an input file called HOTINP. It contains site specific information such as grid variables and digitized ground elevation. The second step (1b) involves running a program called SETHOT which changes nine event specific variables such as time, wind speed, and surface temperature. The input parameters in HOTINP along with a default value for each in brackets are:

**albedg** = ground albedo {0.3}  
**albedt** = canopy albedo {0.1}  
**almax** = maximum leaf surface area density (1./m)  
 {1.}  
**asmax** = maximum non-leaf surface area density (1./m)  
 {0.05}  
**atree** = fractional tree coverage {0.}  
**boweng** = Bowen ratio for ground {0.2}  
**bowmax** = maximum bowen ratio {10.}  
**bowmin** = minimum bowen ratio {-10.}  
**bratio** = Bowen ratio in canopy {1.5}  
**clat** = latitude of grid center {112.}  
**clong** = longitude of grid center {40.10}  
**constr** = constant to approximate fraction of cloud  
 coverage curve {0.8}  
**cs** = specific heat for soil {1256.}  
**delgmt** = time difference between gmt and lst {7.}  
**delt** = time step (sec)  
**deltma** = maximum time step (sec) {999.9}  
**delzr** = delz in added zones (m) enter kadd numbers  
**dqdzadd** = water vapor increment in added layers  
 (g/kg/m) {0.0067}  
**drag** = drag coefficient {0.2}  
**drgmax** = maximum value of drag coefficient {0.50}  
**dtdzadd** = temperature increment in added layers (deg/m)  
 {0.0033}  
**dzdksi** = grid resolution in the surface layer (m) {4.}  
**edksc** = eddy soil conductivity (m\*\*2/s) {4 x 10<sup>-7</sup>}  
**edmax** = maximum eddy viscosity (m\*\*2/s) 500.  
**edmin** = minimum eddy viscosity (m\*\*2/s) .2e-4  
**emissg** = ground emissivity {0.98}  
**excoef** = extinction coefficient {0.6}  
**htree** = height of canopy (m) {18.}  
**iintvl** = i increment for printing {4}  
**imax** = number of cells in x direction {15}  
**jintvl** = j increment for printing {1}  
**jmax** = number of cells in y direction {15}

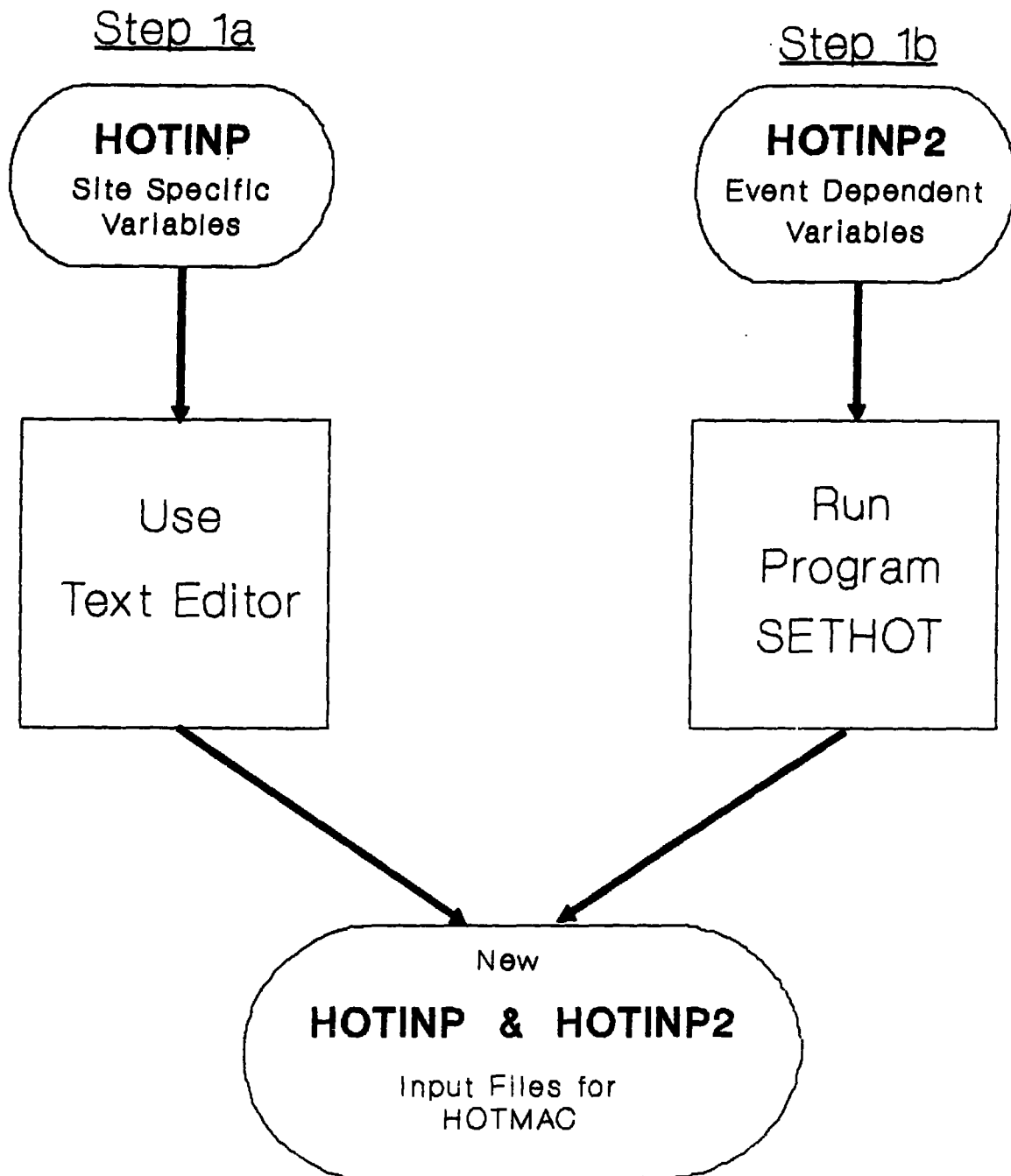
**kadd** = number of cells to add to top in radlon {10}  
**kheit** = height of tree in grid level {4}  
**kintvl** = k increment for printing {1}  
**kmax** = number of cells in z direction {15}  
**ksmax** = number of soil layers {3}  
**ktrans** = top of linear zones {5}  
**ktree** = {2}  
**nlimit** = iteration limit in subroutine "wwind" {15}  
**optpwv** = optical depth of water vapor {3}  
**qminadd** = minimum water vapor in added layers (g/kg/m)  
           {1.}  
**reducu** = velocity scaling factor for u {1.}  
**reducv** = velocity scaling factor for v {1.}  
**relax** = {0.3}  
**rhinit** = initial relative humidity above ground {0.3}  
**rhinit0** = initial relative humidity at ground {0.5}  
**rhos** = soil density {1500.}  
**smooth** = smoothing factor {0.5}  
**tfactor** = {0.025}  
**tolera** = {0.10}  
**topradf** = radiation flux at top of radiation zone  
           (watts/m\*\*2) {200.}  
**treez1** = normalized height of canopy base {0.5}  
**treez2** = normalized height of dead branch base {0.4}  
**utm<sub>x</sub>** = e-w utm position of sw corner (km) {335.}  
**utm<sub>y</sub>** = n-s utm position of sw corner (km) {4420.}  
**xintvl** = x dimension of cell (m) {8000.}  
**yintvl** = y dimension of cell (m) {8000.}  
**zkmaxpl** = maximum height in a terrain following  
           coordinate (m) {5000.}

Figure 2 shows steps 1a and 1b for setting up input for HOTMAC.

Step 1a uses a text editor to change any of the items in HOTINP. Figure 3 shows an example of modifying HOTINP using the "Vi" Text editor.

Step 1b involves the program SETHOT. SETHOT reads in the current HOTINP2 file and writes each variable and its current value on the screen. Typing "sethot" opens a window as shown in Fig. 4. The mouse is used to change values. For example, to read from a different file other than "charlie/Sethot/hotinp2", put the mouse pointer tip to the right of the "2" on the "read from file" line, hit the left button and backspace to

# STEP 1: Set Up Input for HOTMAC:



**Fig. 2.** Two steps for setting up input for HOTMAC.

**STEP 1** Type: \$ vi hotinp

The following text will appear on the screen:

```

                                Grid Variables
'jmax   = number of cells in x direction      '    15.0
'jmax   = number of cells in y direction      '    15.0
'jmax   = number of cells in z direction      '    15.0
'xintv1 = x dimension of cell (m)            '   8000.
'xintv1 = y dimension of cell (m)            '   8000.
'utmx   = e-w utm position of sw corner (km)  '    335.
'utmymy = n-s utm position of sw corner (km)  '   4420.
'clat   = latitude of grid center             '    40.10
'clong  = longitude of grid center            '   112.0
'dzdksi = grid resolution in the surface layer '     4.
'delt   = time step (sec)                     '   900.
'deltma = maximum time step (sec) .           '  999.9
```

**STEP 2** Move blinking cursor( ) to correct position using arrow keys.

Grid Variables

```
'max   = number of cells in x direction      '    15
```

**STEP 3** Erase number by typing an x.

**STEP 4** Type i to get into INSERT MODE and type in new value:

Grid Variables

```
'max   = number of cells in x direction      '    16
```

**STEP 5** Hit the ESC (escape) key to return to COMMAND MODE

**STEP 6** Repeat steps 2 through 5 to make any further changes.

**STEP 7** Type ZZ (shift zz) to write a new version of HOTINP and end the editor session.

Type: quit! to end editor without saving changes.

Fig. 3. Step 1a: Use the Vi editor to modify the file HOTINP.



remove "charlie/Sethot/hotinp2". Once the old file name has been removed, the new one can be typed in. Alternatively, a control "u" could be used to remove the line instead of the backspace key. The full path name, such as "/usr/MDW/Army," should be used. A similar procedure applies to the nine items. Clicking the left button at the appropriate place, permits a new value to be typed. A little more information about each item can be obtained by putting the mouse pointer on the item number and clicking the left button. If an inappropriate entry is made, a box declaring invalid entry will appear which can be removed by correcting the error. Pressing and holding the right button will bring up a box with the entries, "save", "read from file", "save and quit", and "quit without saving". Highlighting an entry and releasing the right button will cause the entry to be executed. For example, selecting "read from file" would cause the entries on the screen to be replaced with those in the file listed on the "read from file" line. Selecting "save and quit" will cause the screen values to be written to the file listed on the "save in file" line, and will terminate sethot.

The file HOTINP2 can also be edited directly. There is only a single entry on each line and they appear in the same order as shown in Fig. 4. Consequently, the synoptic wind direction would be the fourth line of the file.

In summary, Step 1a is performed once to set up HOTINP for a given location. Step 1b is performed to change event dependent variables. In this new way, new versions of HOTINP and HOTINP2 are created and are ready to be used by HOTMAC.

### **Step 2: Run HOTMAC**

To run HOTMAC, type on the keyboard:

HOTMAC (and then hit the enter key). This commands HOTMAC to read in HOTINP and HOTINP2, initialize all the variables, and run for a length of time specified by the variable "comphr" in HOTINP2. At every hour of simulation, new values of wind, temperature, and turbulence, etc., are written to three different output files: HOTOOUT, HOT10, and DIFFIN as shown in Figure 5. When the simulation stops, use a text editor to look at the file HOTOOUT. This is a quick way to check whether the simulation is completed successfully. The file HOT10 is ready to be used as input to HOTPLT.

# SETHOT

## HELP

## VALUE

- |   |         |   |
|---|---------|---|
| 1 Starting Date (Julian)                          | VALUE - | 0 |
| 2 Starting Time (hhmm)                            | VALUE - | 0 |
| 3 Synoptic Wind Speed (m/sec)                     | VALUE - | 0 |
| 4 Synoptic Wind Direction (degrees)               | VALUE - | 0 |
| 5 Temperature at Mean Sea Level (degrees C)       | VALUE - | 0 |
| 6 Linear Profile in Surface Layer (degree K/m)    | VALUE - | 0 |
| 7 Linear Profile in the Upper Levels (degree K/m) | VALUE - | 0 |
| 8 Height Where Profiles Meet (m)                  | VALUE - | 0 |
| 9 Total Computation Duration (hours)              | VALUE - | 0 |

Save in file :

charlie/Sehot/hotinp2

Read from file :

charlie/Sehot/hotinp2

Print

Clear all

Quit

Redisplay

Open all

Tidy

Fig. 4. SETHOT windows.

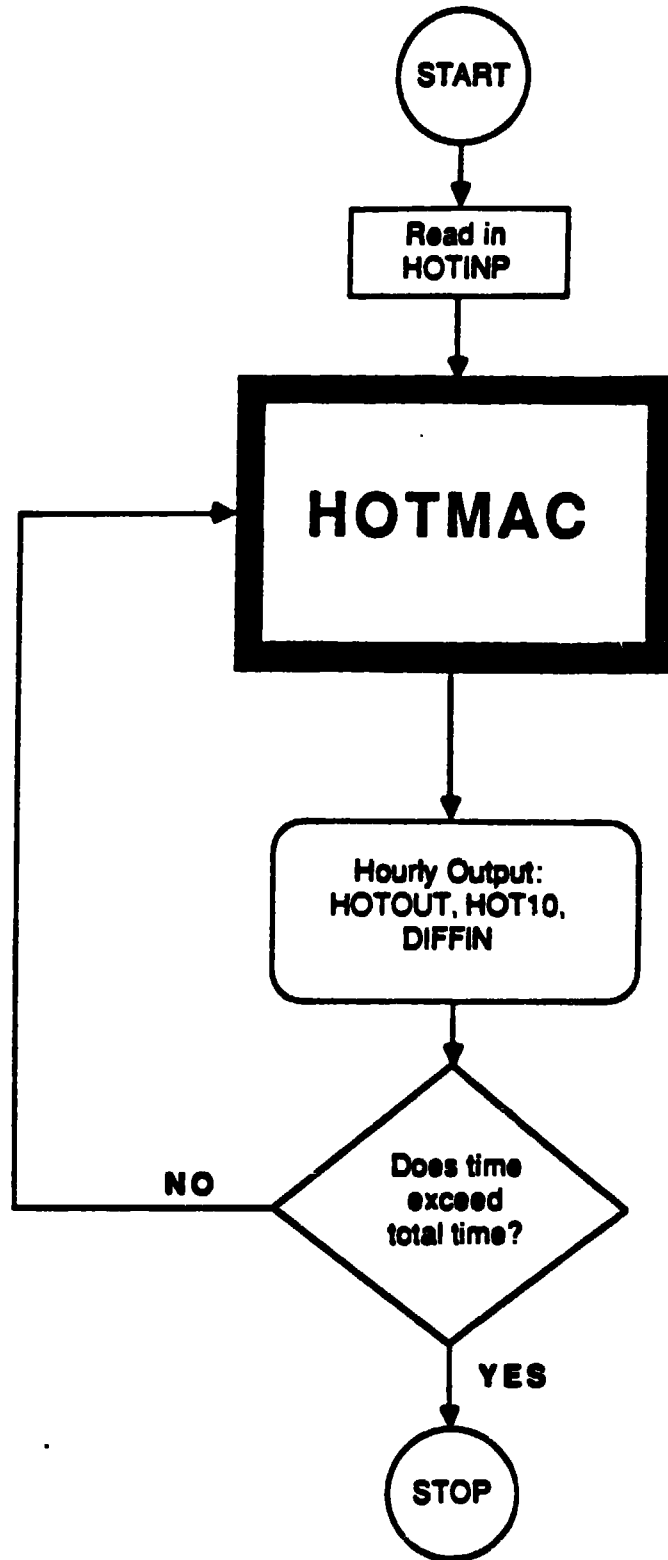


Fig. 5. Flow chart of the program HOTMAC.

### **Step 3 (optional): Run HOTPLT / Produce Plots**

Step 3 is optional and can be accomplished after steps 4, 5, and 6 are completed. Figure 6 shows a schematic of running HOTPLT. HOTPIN has very limited input. It requires the number of wind profile sites desired, NSTN, their station labels, the station locations, and the maximum height above ground, AGLMAX. The station labels are read in a single line with four character names with a leading blank space. The following line is for the UTM easting coordinates expressed in kilometers with free format. The next line gives the UTM northing coordinates. The last line gives AGLMAX, which is the highest height above ground in kilometers at which the profiles are reported. This line is also free format. HOTPIN is modified with the "Vi" editor in a manner similar to that shown for HOTINP in Figure 3.

The various plotting programs, HOTPLT, RAPLOT, and CONPLT, are all designed to display plots rather than print plots. In each case the codes must be run in the NeWS environment. The procedure is to (1) enter the NeWS environment with the command: news, (2) use the right mouse button to bring up a menu and choose a terminal, and (3) type the plotting command, HOTPLT, for example. The program will run and open a window with the first plot displayed upon it. Once the window is opened, any plot in the file can be selected by putting the mouse cursor on the plot window interior and pushing the right mouse button. With the right button held down, a box with the available frames as shown in Figure 7 will appear. The desired frame number can be highlighted with the mouse. Release of the right button causes the desired frame to appear in the window.

Hardcopies of the wind plots can be obtained with the code, HOTPLTP. HOTPLTP constructs meta files for each hour of output and names them as GMETA01, GMETA02, ... GMETA24 for the first, second, and 24<sup>th</sup> hours respectively. The code MULTINP then can be used to send selected plots to the laser printer. For example the command:

```
multinp GMETA23 GMETA02 GMETA10
```

would send the twenty-third, second, and tenth hours of plots to the printer. If too many hours are specified, only the first ones will be actually printed because the printer can store only a limited number. If more than twenty-four hours of simulations are desired a slightly different procedure is required. HOTMAC will actually generate a unformatted

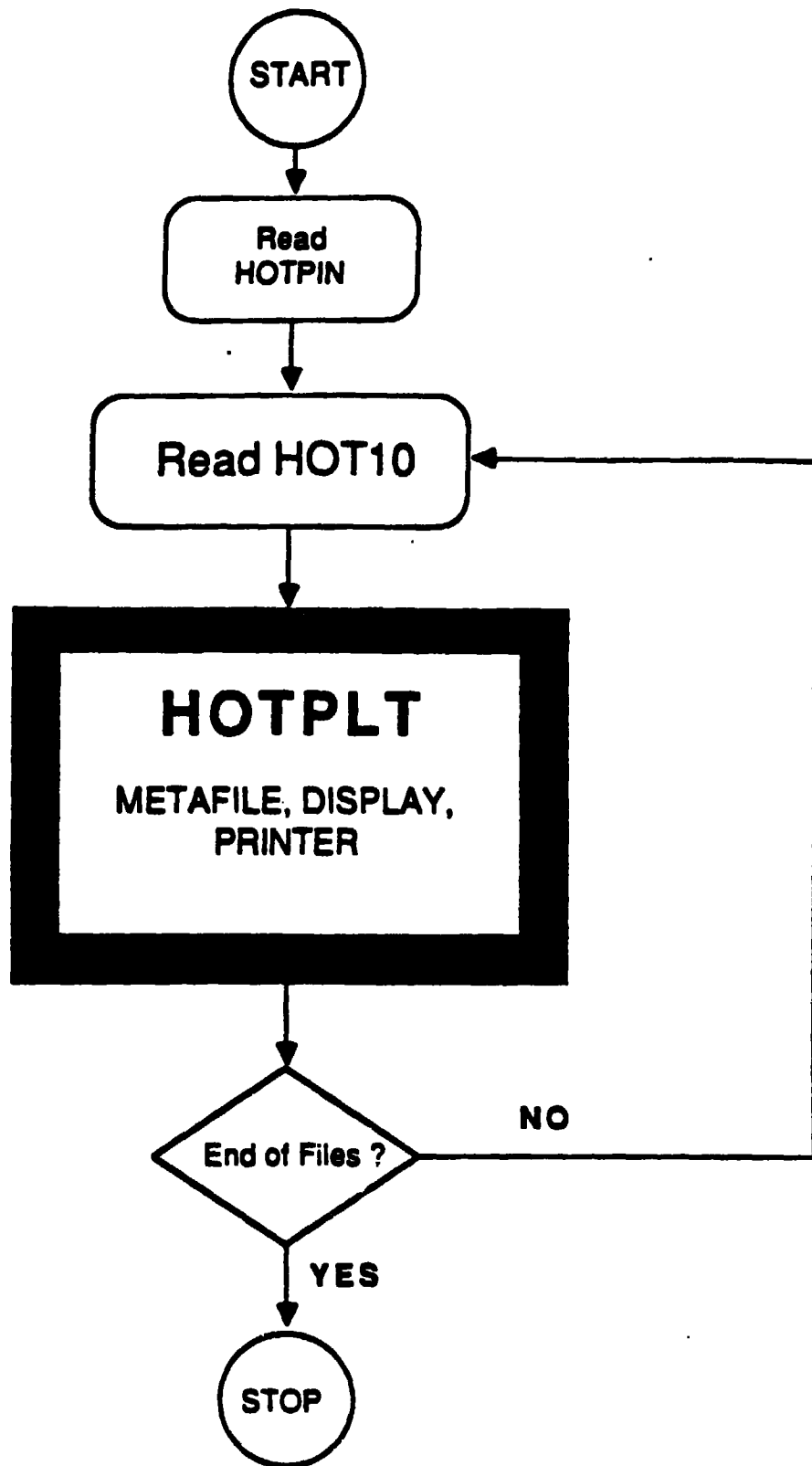


Fig. 6. Flow chart of the program HOTPLT.

height at 6 m  
day 215 2200 1st

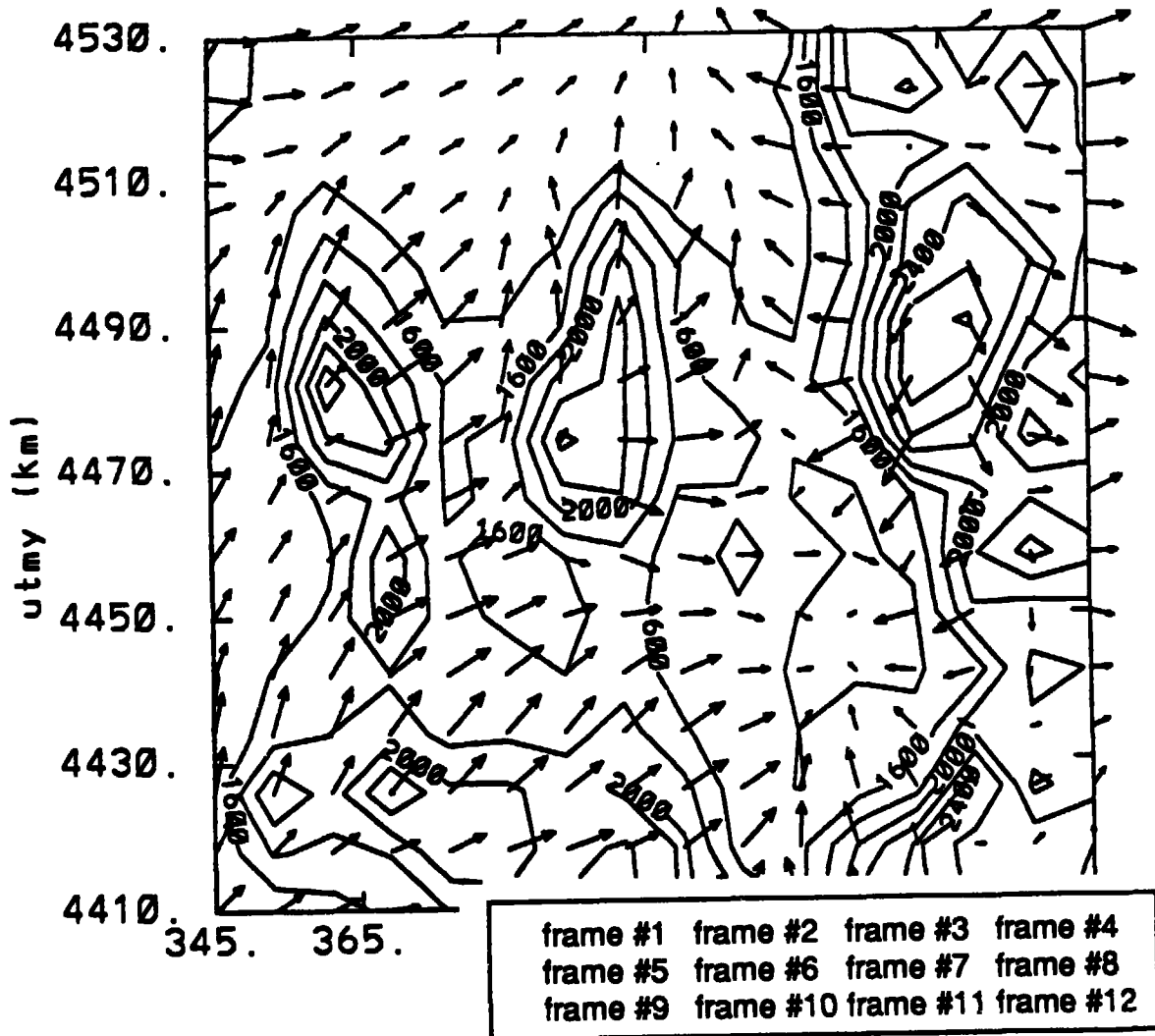


Fig. 7. Plot Selection Screen for HOTPLT

file. HOT10, for each 24 hour period. The first 24 hours will reside on the file HOT10, while the second will reside on the file HOT101, and the third-24 hour segment will be called HOT102. HOTPLT and HOTPLTP each use HOT10 as input, so that the second 24 hour segment would be displayed with the commands:

```
news
cp hot10 hot100
mv hot101 hot 10
hotplt
mv hot10 hot101
```

The plots can be obtained in a similar fashion.

#### **Step 4: Setup Input for RAPTAD**

RAPTAD uses a file called RPIN, which supplies several parameters. The first line provides the parameters: NSKIP, LINTVL, PLUMTIM, DELT, WFACTOR, and CH. These are all read with unspecified format; in the example the names are printed to the right of the variables. The names are not read by the code and are only used as aids to remember the variables.

NSKIP defines the first dump which will be used to interpolate the wind fields to the appropriate times. As an example, consider a simulation of the wind field which was specified as 1800 hours, with a release to be simulated at 2000 hours. HOTMAC provides dumps within a time step beyond each hour. Thus, for time steps of 12 minutes, the first dump would be at 1800 plus delta where delta could be as much as 20 hundredths of an hour. Consequently, the two dumps which would bracket the release time of 2000, would be the second and third dumps and NSKIP would be 2. If the release time were to be 2200 hours the appropriate value of NSKIP would be 4, since the fourth dump would be slightly after 2100 hours while the fifth would be a little after 2200 hours.

LINTVL is used to indicate how many particle-locations and associated parameters will be printed on the debug print file, RPTEST. With LINTVL equal to one, a parameter will be printed for each particle for each hour. For LINTVL greater than one, every LINTVL<sup>th</sup> particle location will be printed.

PLUMTI is the plume time to be simulated in minutes. It is the total time after the start of the release which is to be examined. DELT is the time step in seconds. A short time step is more accurate because the positions of the particles change little during the time step, but a shorter time step, requires more computer time for the same PLUMTI. Too large a time step will allow the particles to traverse too long a distance during a single time step with the result that the assumption that the instantaneous velocities are constant over the time step will be violated. This concern is particularly important for places where the winds are very sensitive to the position, such as very close to the ground where the wind speed changes rapidly with height.

WFACTOR is a factor which adjusts the calculated vertical velocities. A factor larger than one is used to counteract the smoothing of a coarse grid. CH is a horizontal diffusivity factor, which could be used to enhance dispersion.

The second line of input gives the parameters: NDELTP, NP, RMAX, UTMXSO, and UTMYSO. These parameters are read in with unspecified format and are accompanied by their names which are not read. NDELTP provides the number of time steps which are permitted to pass between particle releases within the duration of the release. For example, if DELT were equal to 10 and NDELTP were equal to four, particles would be released at the initial release time and again at 40 seconds later, and at interval of every 40 seconds thereafter until the end of the release period. NP provides the number of particles released at each release time. Typically, NP is put at larger numbers if a very short release is considered. The total number of particles releases is proportional to NP times NDELTP divided by DELT. Larger numbers of particles provide more precise definitions of concentration or dosage fields, but also require more computer time.

RMAX provides the default value of the radius of the cylinder from which particles will be randomly released. The D2 portion of the code will overwrite this value for cases where the radius is defined by the release scenario. UTMXSO and UTMYSO provide the source locations in UTM easting and UTM northing, coordinates, respectively. The values are expressed in kilometers.

The third line in the file provides these parameters: IPSTART, ID2MO, HS, TCUT, and BKGND with unspecified format. IPSTART is the release starting time in hundredths



of an hour, while BKGND is background value for the contaminant which is released. ID2MO is a parameter which allows the user to choose whether or not he will use the D2 source description. If ID2MO is 1, then the D2 subroutine will be entered and the user will be queried as described below. HS is the release height in meters above ground if ID2MO is not 1. TCUT is the duration of the release in seconds, if ID2MO is not 1. If ID2MO is not 1 and an additional line is inserted between lines 3 and 4 which gives XMWT, the molecular weight of the species. Without the use of D2 the final concentrations will be in parts per trillion and will be appropriate to an emission rate of 1 gram per second. With ID2MO equal to 1, the concentrations are given in milligrams per cubic meter.

The fourth line in the file provides: NSITE and IDS(n). NSITE is the number of sites for which a time series of dosage or concentration is desired while IDS(ns) are the NSITE station labels. The format is (9x,i1,9x,7(a4,1x)).

The fifth and sixth lines provide the sampling sites UTM easting and northing coordinates respectively. These data are expressed in kilometers; the first six characters describe the variable (SUTMX or SUTMY) while the remaining numbers are in free format.

This file is most easily constructed by using the Vi editor to edit the example shown in Figure 8. However SETRAP can be used to modify RPIN.

```

3, 1, 180., 10., 1.5, 0.      nskip, lintvl, plumtim, delt, wfactor, ch
8, 1, 5.0, 83.80, 61.50      ndeltp, np, rmax, utmaxso, utmyso
1700, 0., 50., 10800., 0.5   ipstart, id2mo, hs, tcut, bkgnd
146.1, xmwt
nsite = 2, ids = grm, stp
klev = 2, 2
samptiin = 60., 60
bdz = 1., 1.
sutmx = 84.0, 84.0
sutmy = 63.0, 67.0

```

Fig. 8. Example of file RPIN

SETRAP must be run in a NeWS window and it requires that a map image be available. Once SETRAP is typed in, a window similar to that of Fig. 9 appears.

The mouse can then be used to select an item to be changed or to locate the position of the release. When the cursor is placed on the map portion of the window, clicking

**Fig. 9. SETRAP window.**

the left button changes the release position. The release coordinates can also be changed by moving the mouse pointer to the new value box opposite the one showing the release position and clicking the left button and typing in the desired values. If old values are present which need to be erased, the mouse pointer can be placed to the right of the entry to be erased. Clicking the left button permits the backspace key to be used to erase the entry. Alternatively, the control "u" command can be used to erase the line. In a similar fashion, the start time for the release, duration of the release, and time step can also be changed.

Clicking the right button brings up a box with the entries, "done," "cancel," and "zap." To write the modifications to RPIN, hold the right button down and highlight the entry "done"; releasing the right button causes the corrections to be written to RPIN and finishes SETRAP.

All of the entries in RPIN can also be edited directly, so that SETRAP is not essential.

### **Step 5: Run RAPTAD**

Figure 10 describes the fifth step. RAPTAD uses wind and turbulence information from DIFFIN to compute the locations of each particle released. RAPTAD also computes the plume concentrations every 15 minutes. At the end of every hour, particle locations and plume concentrations are written to output files called PARTCL and CONCEN and are then available for plotting. RAPTAD continues with the next hour of computation until the total simulation time is reached.

RAPTAD has been written to call an existing computer code called D2 as a subroutine. Figure 11 gives an example of the questions D2 writes to the screen.

The terminal input begins when the program asks for a novice level. A "0" means that a person is an expert and needs no explanation, where "1" provides a single line of possible responses from which to choose. The choice of "2" provides more explanation and is a good choice for a beginner.

The second question asks for a munition type. For stack sources "non," which means not specified, must be used. The next line asks for an agent type such as "gb." The next two questions are about the type and length of release. For a buoyant stack plume,

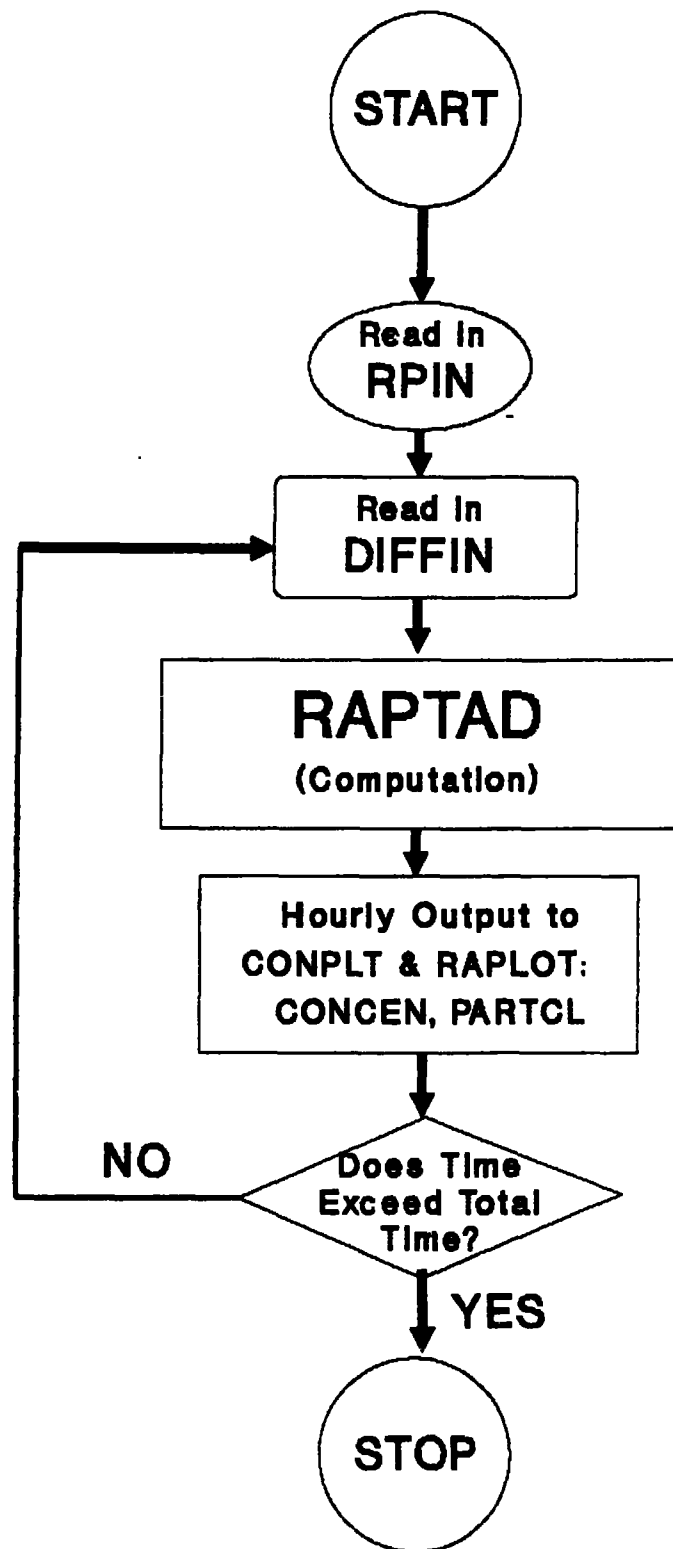


Fig. 10. Flow chart of the program RAPTAD.

```

<mdw> % raptad
Copyright, 1988, The Regents of the University of California
This software was developed pursuant to Contract No.
w-7405-ENG-36 between the U. S. Department of
Energy and The Regents of The University of California
press= 838.0 pmm= 838.0

-----
| downwind hazard program d2pc |
-----

type ? for definitions

1. your novice level: 3,2,1 or 0 nov
input:
2

5. munition type          mun
    105    105-mm cartridge,m60,m360
    155    155-mm projectile,m110,m121a1
    8in    8-inch projectile,m126
    500    500-lb bomb,mk94
    750    750-lb bomb,mc-1
    m55    115-mm rocket,m55
    525    525-lb bomb,mk116
    139    bomblet,m139
    m23    land mine,m23
    4.2    4.2-inch cartridge,m2a4
    non    nonmunition

input:

```

Fig. 11. User interface questions and possible answers regarding the source characteristics.

non

6. agent type	agn
ga tabun	h1 hn-1,nitrogen mustard
gb sarin	h3 hn-3,nitrogen mustard
gd soman	ht 60% hd & 40% t
gf ea 1212	ll lewisite
vx ea 1701	ac hydrogen cyanide
bz incap agent	cg phosgene
hy hydrazine	ck cyanogen chloride
ud udmh	dm adamsite
hd distilled mustard	na not an agent

input:

gb

8. release type	rel
ins	instantaneous(explosive)
evp	evaporation from a puddle formed by a spill
sem	uniform release for afinite time
var	source defined as a number of uniform releases(max 6)
stk	release of heated effluent from stack
stj	release from stack with jet effect
fls	flash fire from ground level
fir	fire burning for finite time
igl	m55 igloo fire
evs	evaporation in still air

input:

Fig. 11. cont.

stk

di= 0.5 6.0 10.0

13. nqi, q() (mg), tq() (min)

nqi number of time intervals

q() source for each interval

tq() cumulative time from beginning of first

input:

1, 3600000, 60

all other input

all

1 mun:non agn:gb rel:stk wnd= 0.4(m/s) tmp=19.5(c) - stb:

24. height of stack (m) hst

input:

10.

25. diameter of stack (m) dst

input:

1.

26. temperature of stack (deg c) tst

input:

25.

27. velocity of effluent (m/sec) vst

input:

Fig. 11. cont.

```

input:
20.

28. relative density of effluent rde
input:
.98
all other input
all

1 mun:non agn:gb rel:stk wnd= 0.4(m/s) tmp=19.5(c) - stb:
24. height of stack (m) hst 10.00
25. diameter of stack (m) dst 1.00
26. temperature of stack (deg c) tst 25.00
27. velocity of effluent (m/sec) vst 20.00
28. relative density of effluent rde 0.98
all other input
stp

```

Fig. 11. cont.

the release type should be "stk." An example entry, for source period, total emission in milligrams for each period, and the period length in minutes is "2, 1000000, 60, 200000, 45." This would represent a total of two periods, with the first one lasting 60 minutes with a total emission of 1000 grams and the second lasting 45 minutes with a total emission of 200 grams.

The next line asks "all other input." If the input is not complete, for example with stack sources where the stack parameters have not yet been entered, the response should be "all."

The next five questions involve the height and diameter of the stack, and the temperature, velocity, and relative density of the effluent. Finally, the code asks "all other input" for which a response of "all" is appropriate. The code will ask the same question



again for which a response of "stp" for stop is required.

### **Step 6: Running Conplt/Produce Contour Plots**

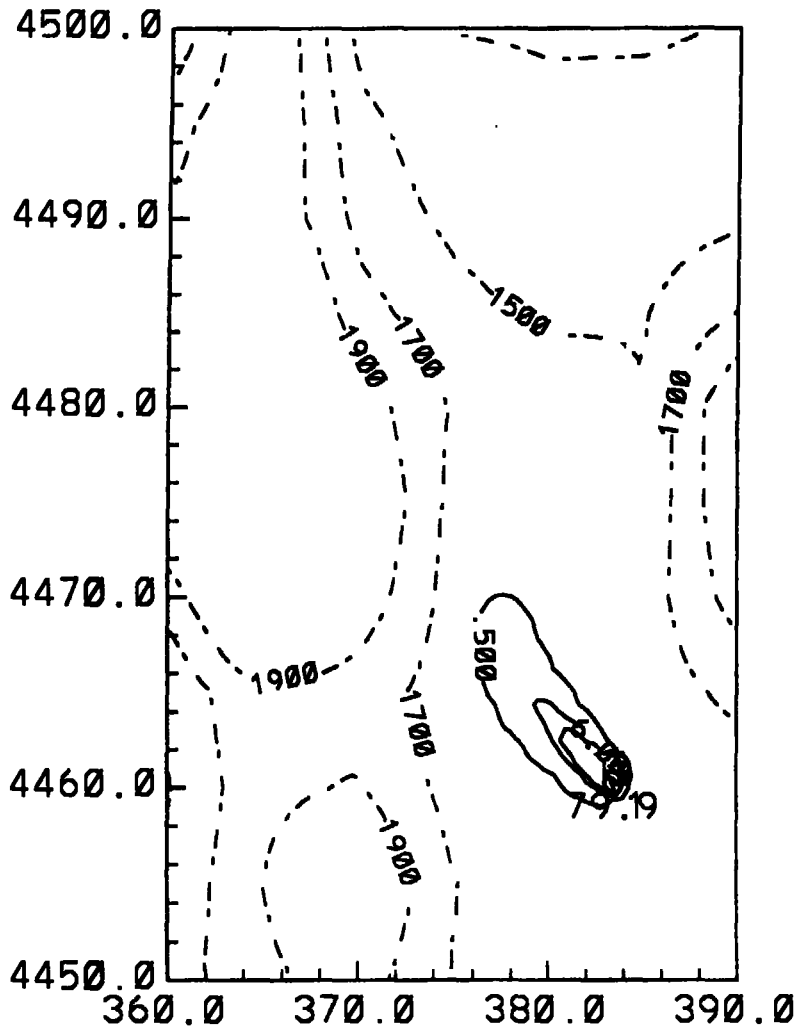
CONPLT uses a single input file CONINP, beyond CONCEN which is produced by RAPTAD. CONINP has only the parameter SCALEF. SCALEF multiplies the concentrations to provide concentration appropriate to other emission rates. CONPLT requires only the command "conplt" to execute, although it must be given in the NeWS environment. Upon completion, the first contour plot will appear on the screen. Additional plots can be shown by using the mouse to bring up the frame menu and highlight the appropriate frame as described in Step 3. Hard copies may be obtained by the command "multinp GMETA." Figure 12 displays an example of the dosage contours produced by CONPLT, while Fig. 13 is an example of the time - dosage plots produced by CONPLT.

### **Step 7. (Optional) Running RAPLOT**

RAPLOT requires an input file called PLMINP. The first line of PLMINP provides the number of stations which will be plotted on the map with the particle locations. Free format is used. The second line provides the labels for each of the stations; the format is (7(1x,a4)). The third and fourth lines give the UTM easting and UTM northing locations, respectively, for each station. The locations are expressed in kilometers and are read with free format. Once again the Vi editor is used to adjust the values in a fashion similar to that used for HOTINP.

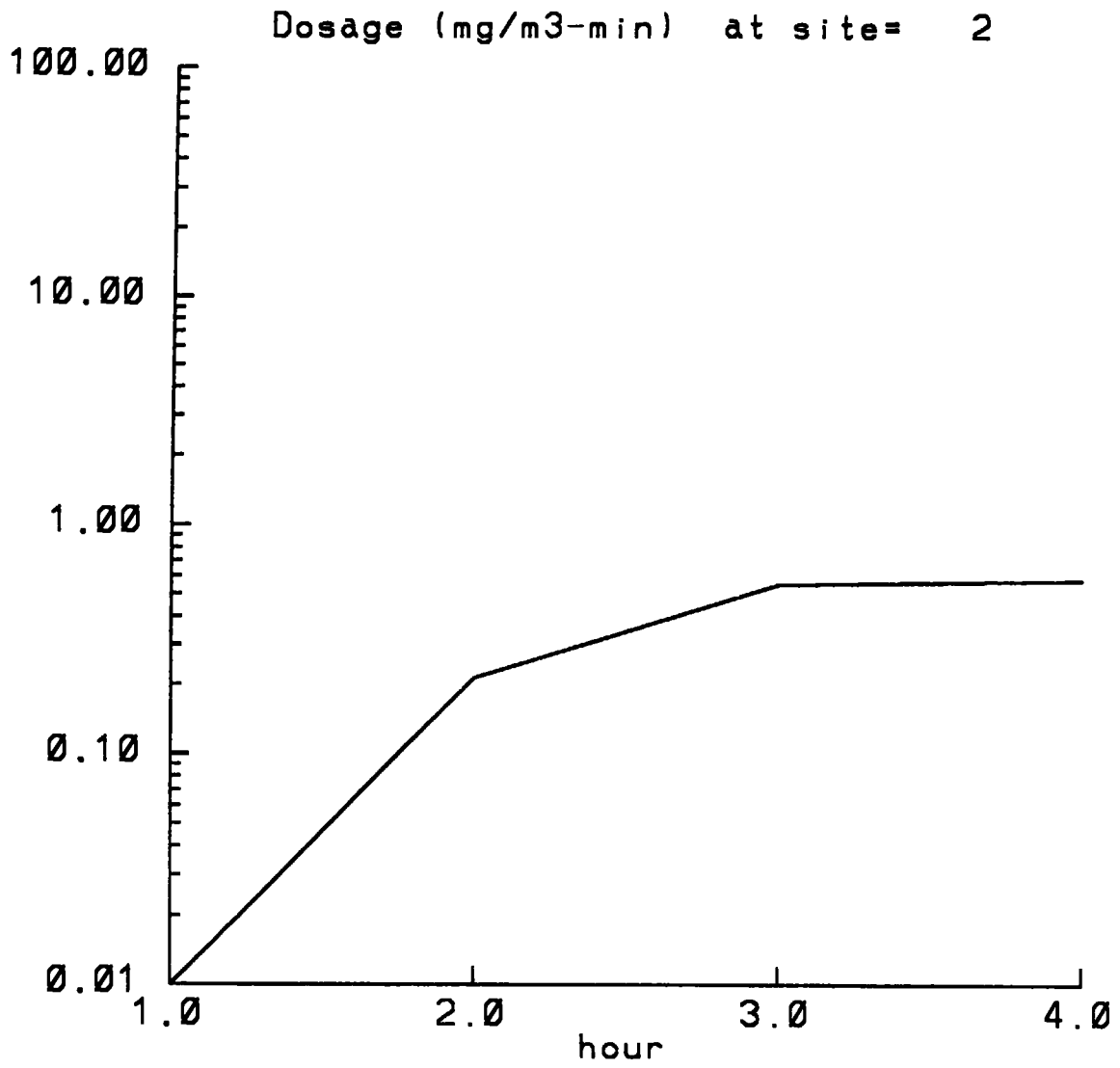
RAPLOT is executed by the command "RAPLOT" which must be given in the NeWS environment. Upon completion the first plot will appear with the particle positions superimposed on the terrain. Desired plots can be shown with the mouse as described in Step 3. Hard copies may be obtained with the command "multinp GMETA." Figure 14 is an example of the particle location plots produced by RAPLOT.

Dosage Contours (mg/m<sup>3</sup>-min) for hour= 3



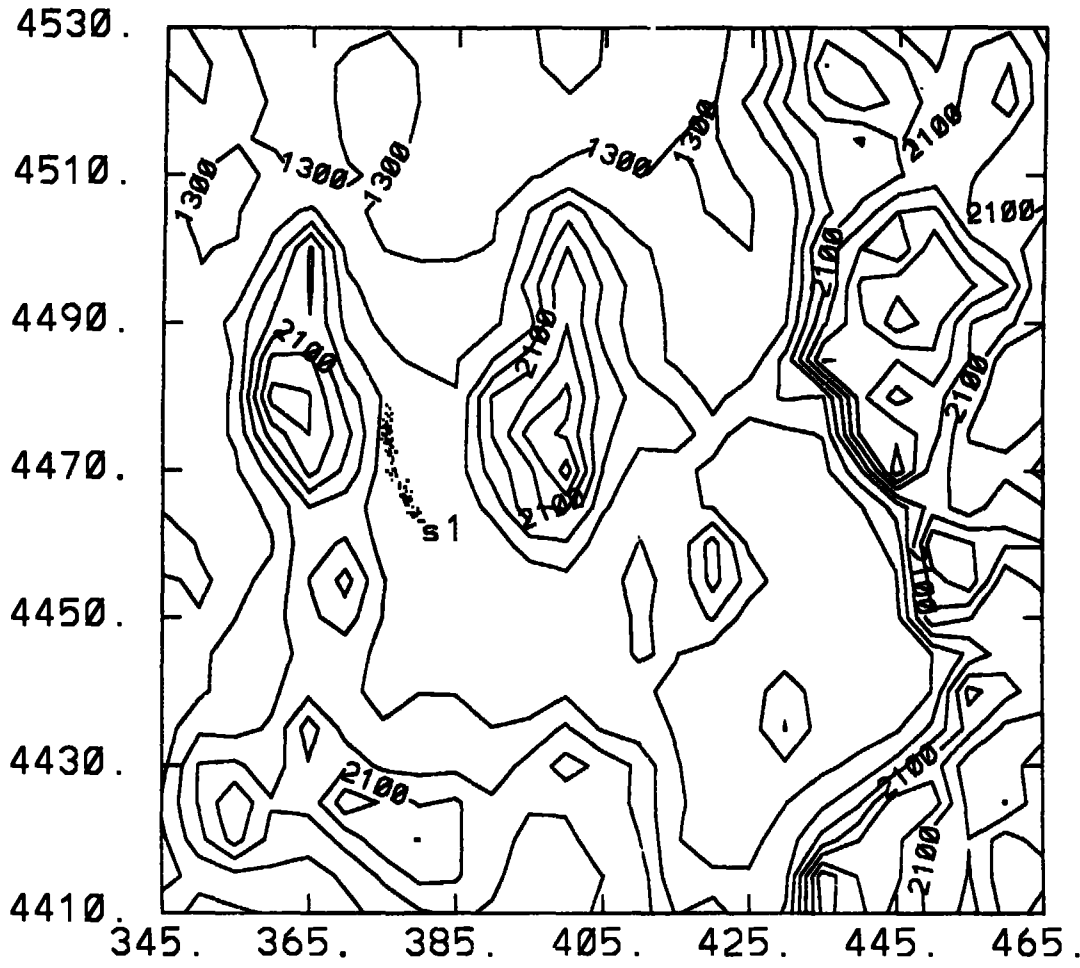
JR FROM 10.000 TO 0.100000E+06 CONTOUR INTERVAL OF 99990. PT(3,3)= 0. LABELS SCALED BY 0.1000

Fig. 12. Dosage contours produced by CONPLT for a 750 pound bomb explosion.



**Fig. 13.** Time-dosage profiles produced by CONPLT.

time: 104 hrs age of plume, 2 hrs  
 age of plume, 2 hrs  
 no. of particles released: 120



CONTOUR FROM 100.00 TO 2900.0 CONTOUR INTERVAL OF 200.00 PT(3,3)= 2170.0

Fig. 14. Pseudo-particle locations depicted by RAPLOT.

### III. DESCRIPTION OF MODELS

#### A. HOTMAC (Higher Orders Turbulence Model for Atmospheric Circulation)

**Model Equations.** This model, also referred to as a "second-moment turbulence-closure model," is based on a set of second-moment turbulence equations closed by assuming certain relationships between unknown higher-order turbulence moments and the known lower-order variables. The model output variables are winds, potential temperature, mixing ratios of water vapor and liquid water, turbulence second moments, a turbulence length scale, and turbulence transport coefficients (eddy viscosity and eddy diffusivity). These results can be used as inputs to pollutant dispersion models. The model is time dependent and three-dimensional in space.

HOTMAC can be used under quite general conditions of flow and thermal stratification: methods for turbulence parameterization are more advanced than those in simple eddy viscosity models. The present model, combined with a statistical cloud model, has simulated interaction between water phase changes and basic dynamic variables. For example, computed turbulence energy increases substantially in the layers where condensation occurs. This appears reasonable, since the latent heat released by condensation produces local unstable layers, resulting in generation of turbulence. Effects of short- and long-wave solar radiation, tall tree canopies, and topography are also included in the model. Surface temperatures are computed from a heat conduction equation for the soil and a heat energy balance equation at the surface.

The present model assumes hydrostatic equilibrium and uses the Boussinesq approximation. Therefore, in theory, the model applications are limited to flows where the local acceleration and advection terms in the equation of vertical motion are much smaller than the acceleration due to gravity (hydrostatic equilibrium) and temperature variations in the horizontal are not too large (Boussinesq approximation).

The model has been used for a variety of fluid problems: surface boundary layer (Mellor, 1973), atmospheric boundary layer, (Mellor and Yamada, 1974; Yamada and Mellor, 1975; Yamada, 1975; Yamada and Mellor, 1979; Yamada and Kao, 1986), airflow over tall tree canopies (Yamada, 1982), air pollution transport (Yamada, 1977), ocean boundary layer, (Mellor and Durbin, 1975), airflow over a cooling pond (Yamada, 1979), laboratory

flows (Briggs, Mellor, and Yamada, 1977), flow over complex terrain (Yamada, 1983), and the results have been used in dispersion simulations over complex terrain (Yamada, 1981; Yamada and Bunker, 1987), over the eastern half of the U.S. (Kao and Yamada, 1987) and over the mountainous western U.S. (Yamada et al. 1987b). This model has also been used by others including Dobosy (1979), Shaw (1977), Burk (1977), Miyakoda and Sirutis (1978), Freeman (1977), and Sun and Ogura (1979). A complete summary of the model is given in a recent review paper (Mellor and Yamada, 1982).

The basic equations of HOTMAC for mean wind, temperature, mixing ratio of water vapor, and turbulence are similar to those used by Yamada (1981, 1985), except two improvements, the nested grid capability and effects of shadows produced by terrain, are added.

A terrain-following vertical coordinate system is used in order to increase the accuracy in the treatment of surface boundary conditions:

$$z^* = \bar{H} \frac{z - z_g}{H - z_g}, \quad (1)$$

where  $z^*$  and  $z$  are the transformed and Cartesian vertical coordinates, respectively;  $z_g$  is ground elevation;  $\bar{H}$  is the material surface top of the model in the  $z^*$  coordinate; and  $H$  is the corresponding height in the  $z$ -coordinate.

The governing equations, following the coordinate transformation, are (Yamada, 1981)

$$\begin{aligned} \frac{DU}{Dt} = & f(V - V_g) + g \frac{\bar{H} - z^*}{\bar{H}} \left( 1 - \frac{\langle \Theta_v \rangle}{\Theta_v} \right) \frac{\partial z_g}{\partial x} \\ & + \frac{\partial}{\partial x} \left( K_x \frac{\partial U}{\partial x} \right) + \frac{\partial}{\partial y} \left( K_{xy} \frac{\partial U}{\partial y} \right) + \frac{\bar{H}}{H - z_g} \frac{\partial}{\partial z^*} (-\bar{u}w) \end{aligned} \quad (2)$$

$$\begin{aligned} \frac{DV}{Dt} = & -f(U - U_g) + g \frac{\bar{H} - z^*}{\bar{H}} \left( 1 - \frac{\langle \Theta_v \rangle}{\Theta_v} \right) \frac{\partial Z_g}{\partial y} \\ & + \frac{\partial}{\partial x} \left( K_{xy} \frac{\partial V}{\partial x} \right) + \frac{\partial}{\partial y} \left( K_y \frac{\partial V}{\partial y} \right) \\ & + \frac{\bar{H}}{H - z_g} \frac{\partial}{\partial z^*} (-\bar{v}w) \end{aligned} \quad (3)$$

$$\frac{\partial U}{\partial x} + \frac{\partial V}{\partial y} + \frac{\partial W^*}{\partial z^*} - \frac{1}{H - z_g} \left( U \frac{\partial z_g}{\partial x} + V \frac{\partial z_g}{\partial y} \right) = 0 , \quad (4)$$

where

$$W^* \equiv \frac{\bar{H}}{H - z_g} W + \frac{z^* - \bar{H}}{H - z_g} \left( U \frac{\partial z_g}{\partial x} + V \frac{\partial z_g}{\partial y} \right) \quad (5)$$

and

$$\frac{D(\quad)}{Dt} \equiv \frac{\partial(\quad)}{\partial t} + U \frac{\partial(\quad)}{\partial x} + V \frac{\partial(\quad)}{\partial y} + W^* \frac{\partial(\quad)}{\partial z^*} . \quad (6)$$

In the above expressions,  $\langle \rangle$  indicates an average over a horizontal surface. The second terms on the right-hand side of Eqs. (2) and (3) indicate the effects of ground slope. For simplicity,  $H$  is specified as

$$H = \bar{H} + z_{gmax} , \quad (7)$$

where  $z_{gmax}$  is the maximum value of the ground elevation in the computational domain.

The geostrophic winds  $U_g$  and  $V_g$  are computed from Yamada (1981), i.e.,

$$\begin{aligned} fU_g \equiv & fU_g(\bar{H}) \frac{\langle \Theta_v \rangle}{\langle \Theta_v(\bar{H}) \rangle} + g \frac{H - z_g}{\bar{H}} \int_{z^*}^{\bar{H}} \frac{1}{\langle \Theta_v \rangle} \frac{\partial}{\partial y} \Delta \Theta_v dz' \\ & - \frac{g}{\bar{H}} \frac{\partial z_g}{\partial y} \int_{z^*}^{\bar{H}} \frac{\Delta \Theta_v}{\langle \Theta_v \rangle} dz' , \end{aligned} \quad (8)$$

and

$$\begin{aligned} fV_g \equiv & fV_g(\bar{H}) \frac{\langle \Theta_v \rangle}{\langle \Theta_v(\bar{H}) \rangle} - g \frac{H - z_g}{\bar{H}} \int_{z^*}^{\bar{H}} \frac{1}{\langle \Theta_v \rangle} \frac{\partial \Delta \Theta_v}{\partial x} dz' \\ & + \frac{g}{\bar{H}} \frac{\partial z_g}{\partial x} \int_{z^*}^{\bar{H}} \frac{\Delta \Theta_v}{\langle \Theta_v \rangle} dz' , \end{aligned} \quad (9)$$

where  $\Delta \Theta_v \equiv \Theta_v - \langle \Theta_v \rangle$ , and the abbreviated symbols  $U_g(\bar{H}) \equiv U_g(x, y, \bar{H}, t)$ .  $V_g(\bar{H}) \equiv V_g(x, y, \bar{H}, t)$ , are used. The derivations of Eqs. (2) to (5), (8), and (9) are given in the Appendix of Yamada (1981). A turbulence kinetic energy equation is given by

$$\begin{aligned}
\frac{D}{Dt} \left( \frac{q^2}{2} \right) &= \frac{\partial}{\partial x} \left[ K_x \frac{\partial}{\partial x} \left( \frac{q^2}{2} \right) \right] - \frac{\partial}{\partial y} \left[ K_y \frac{\partial}{\partial y} \left( \frac{q^2}{2} \right) \right] \\
&+ \left( \frac{\bar{H}}{H - z_g} \right)^2 \frac{\partial}{\partial z^*} \left[ q \ell S_q \frac{\partial}{\partial z^*} \left( \frac{q^2}{2} \right) \right] \\
&- \frac{\bar{H}}{H - z_g} \left( \overline{u w} \frac{\partial U}{\partial z^*} + \overline{v w} \frac{\partial V}{\partial z^*} \right) \\
&+ \beta g \overline{w \theta_v} - \frac{q^3}{B_1 \ell} ,
\end{aligned} \tag{10}$$

and a turbulence length scale  $\ell$  is obtained from

$$\begin{aligned}
\frac{D}{Dt} (q^2 \ell) &= \frac{\partial}{\partial x} \left[ K_x \frac{\partial}{\partial x} (q^2 \ell) \right] + \frac{\partial}{\partial y} \left[ K_y \frac{\partial}{\partial y} (q^2 \ell) \right] \\
&+ \left( \frac{\bar{H}}{H - z_g} \right)^2 \frac{\partial}{\partial z^*} \left[ q \ell S_\ell \frac{\partial}{\partial z^*} (q^2 \ell) \right] \\
&- \ell F_1 \left[ \frac{\bar{H}}{H - z_g} \left( -\overline{u w} \frac{\partial U}{\partial z^*} - \overline{v w} \frac{\partial V}{\partial z} \right) + \beta g \overline{w \theta_v} \right] \\
&- \frac{q^3}{B_1} \left[ 1 + F_2 \left( \frac{\ell}{kz} \right)^2 \right] ,
\end{aligned} \tag{11}$$

where  $q^2 = \overline{u^2} + \overline{v^2} + \overline{w^2}$  is twice the turbulence kinetic energy,  $\overline{w \theta_v}$  turbulence heat flux,  $\theta_v$  the fluctuation part of virtual potential temperature, and  $(F_1, F_2, S_q, S_\ell, \text{ and } B_1) = (1.8, 1.33, 0.2, 0.2, \text{ and } 16.6)$ , empirical constants determined from laboratory experiments (Mellor and Yamada, 1982). The internal heat energy equation is written as in Yamada and Bunker (1989)

$$\begin{aligned}
\frac{D \Delta \Theta}{Dt} &= \frac{\partial}{\partial x} \left[ K_x \frac{\partial \Delta \Theta}{\partial x} \right] + \frac{\partial}{\partial y} \left[ K_y \frac{\partial \Delta \Theta}{\partial y} \right] + \frac{\bar{H}}{H - z_g} \\
&\times \left[ \frac{\partial}{\partial z^*} (-\overline{w \theta}) + \frac{1}{\rho C_p} \frac{\partial R_N}{\partial z^*} - W \frac{\partial \Theta_v}{\partial z} \right] ,
\end{aligned} \tag{12}$$

The long-wave radiation flux  $R_N / \rho C_p$  is computed according to Sasamori (1968). A conservation equation for mixing ratio of water vapor is given by



$$\frac{DQ_v}{Dt} = \frac{\partial}{\partial x} \left[ K_x \frac{\partial Q_v}{\partial x} \right] + \frac{\partial}{\partial y} \left[ K_y \frac{\partial Q_v}{\partial y} \right] + \frac{\bar{H}}{H - z_g} \frac{\partial}{\partial z^*} (-\overline{wq_v}) . \quad (13)$$

The turbulent fluxes in Eqs. (2), (3), (10), (11), (12), and (13) are obtained from simplified second-moment turbulence-closure equations (Yamada 1983):

$$(\overline{uw}, \overline{vw}) = -\ell q \tilde{S}_M \left[ \frac{\partial U}{\partial z}, \frac{\partial V}{\partial z} \right] \quad (14a, b)$$

$$(\overline{w\theta}, \overline{wq_v}) = -\alpha \ell q \tilde{S}_M \left[ \frac{\partial \Theta}{\partial z}, \frac{\partial Q_v}{\partial z} \right] \quad (15a, b)$$

where  $\tilde{S}_M$  and  $\alpha$  are functions of the flux Richardson number, and  $\alpha (\equiv K_H/K_M$  where  $K_H$  is an eddy diffusivity coefficient and  $K_M$  is an eddy viscosity coefficient) is the reciprocal of the turbulent Prandtl number.

The expressions for  $\tilde{S}_M$  and  $\alpha$  were obtained from the level 2 model of Mellor and Yamada (1974) where temporal and spatial derivatives in Eq. (10) are neglected. The readers are referred to Yamada (1975) for further discussions of the level 2 model equations. The final expressions for  $\tilde{S}_M$  and  $\alpha$  are given in Yamada (1983) and are not repeated here.

**Boundary Conditions.** Surface boundary conditions for (2), (3), and (10) to (13) are constructed from the empirical formulas by Dyer and Hicks (1970) for the nondimensional wind and temperature profiles [see the Appendix of Yamada (1981)]. Strictly speaking, the formulas are valid only for horizontally homogeneous surfaces. It is assumed, however, that the same relations are fair approximations over nonhomogeneous terrain, provided that the formulas are applied sufficiently close to the surface. It should be noted that vegetation plays an active part in the apportionment of available heat energy between convective (sensible and latent) and conductive (into the soil) components. Use of the similarity formulas requires knowledge of the surface temperatures; a method to obtain the surface temperature is discussed below.

The temperature  $T_s$  in the soil layer is obtained by solving the heat conduction equation

$$\frac{\partial T_s}{\partial t} = \frac{\partial}{\partial z_s} \left( K_s \frac{\partial T_s}{\partial z_s} \right) , \quad (16)$$

where  $z_s$  is positive downward, and soil diffusivity  $K_s$  can be a function of soil moisture content. Appropriate boundary conditions for solution of Eq. (16) are the heat energy balance at the soil surface and specification of the soil temperature or soil heat flux at a certain depth whose value is dependent on the duration of the integration. The heat energy balance at the surface is given by

$$R_s + R_L \downarrow - R_L \uparrow = H_s + LE + G_s , \quad (17)$$

where  $R_s$  is the incoming direct solar radiation absorbed by the surface,  $R_L \downarrow$  is the incoming long-wave radiation, and  $R_L \uparrow$  is the outgoing long-wave radiation.

The surface heat flux  $H_s$ , latent heat flux  $LE$ , and ground heat flux  $G_s$  are given by

$$H_s = -\rho_a c_p u_* T_* , \quad (18)$$

$$LE = -\rho_a L u_* Q_* , \quad (19)$$

and

$$G_s = K_s \left. \frac{\partial T_s}{\partial z_s} \right|_G , \quad (20)$$

where  $\rho_a$  is the air density,  $u_*$  is the friction velocity,  $T_*$  is the temperature scale,  $Q_*$  is the water vapor scale, and the subscript  $G$  denotes the value at the ground surface. Substituting (18) to (20) into (17) we obtain

$$R_s + \epsilon R_L \downarrow - \epsilon \sigma T_G^4 = -\rho_a c_p u_* T_* (1 + B^{-1}) - K_s \partial T_s / \partial z_s |_G , \quad (21)$$

where the relation

$$R_L \uparrow = \epsilon \sigma T_G^4 + (1 - \epsilon) R_L \downarrow , \quad (22)$$

and Bowen ratio

$$B = H_s / LE , \quad (23)$$

are used;  $\epsilon$  is the emissivity of the surface and  $\sigma$  is the Stefan-Boltzman constant. Garratt and Hicks (1973) obtained a relationship between the surface temperature and air temperature at  $z_1$  (in the surface layer):

$$(\Theta(z_1) - \Theta_G)T_*^{-1} = (P_r/k)[\ln\{(z_1 + z_{ot})/z_o\} + \ln(z_o/z_{ot}) - \psi] , \quad (24)$$

where  $P_r$  is the turbulence Prandtl number at neutral stability,  $k$  is the von Karman constant,  $z_o$  and  $z_{ot}$  are the roughness lengths for momentum and temperature, and  $\psi$  is the stability correction terms of Panofsky (1963). A constant value of 0.1 m is assumed for  $z_o$ , and  $z_{ot}$  is obtained from a relationship  $\ln(z_o/z_{ot}) = 2$  (Garratt and Hicks, 1973). Using Eq.(24) we can eliminate  $T_*$  from Eq. (21) to obtain

$$R_s + \epsilon R_L \downarrow - \epsilon \sigma T_G^4 + m[\Theta(z_1) - T_G(P_o/P_G)^{R/c_p}] + K_s \left. \frac{\partial T_s}{\partial z_s} \right|_G = 0 , \quad (25)$$

where

$$m = k\rho_a c_p u_* (1 + B^{-1}) P_r^{-1} [\ln\{(z_1 + z_{ot})/z_o\} + 2 - \psi]^{-1} \quad (26)$$

$P_o$  is a reference pressure (1000 mb) and  $P_G$  is the pressure at the surface. Equation (25) may be linearized by noting that

$$(T_G^{n+1} - T_G^n)/T_G^n \ll 1$$

where the superscripts  $n$  and  $n + 1$  denote the  $n$  and  $(n + 1)^{th}$  time steps of integration (a typical time increment used in integration is 1 minute). After substitution into Eq. (25) of the approximation

$$(T_G^{n+1})^4 \approx 4(T_G^n)^3 T_G^{n+1} - 3(T_G^n)^4 , \quad (27)$$

we obtain

$$\left[ 4\epsilon\sigma(T_G^n)^3 + m(P_o/P_G)^{R/c_p} + \frac{K_s}{\Delta z_s} \right] T_G^{n+1}$$

$$\begin{aligned}
&= \left( \frac{K_s}{\Delta z_s} \right) T_s^{n+1}(1) + R_s + \epsilon R_L \downarrow \\
&+ 3\epsilon\sigma(T_G^n)^4 + m\Theta^n(z_1) , \tag{28}
\end{aligned}$$

where the derivative  $\partial T_s / \partial z_s$  at  $z_G$  is replaced by a forward finite-difference approximation  $(T_s^{n+1}(1) - T_G^{n+1}) / \Delta z_s$ ,  $T_s(1)$  is the soil temperature at the first grid level from the surface, and  $\Delta z_s$  is the distance between the surface and the first grid level in the soil layer.

Equation (16) is solved numerically in finite-difference form by Laasonen (Richtmyer and Morton, 1967, p. 189). By this method Eq. (16) reduces to  $AT_s = B$  where  $A$  is a tridiagonal matrix and  $B$  is a column vector. The solution is conveniently obtained by using the relation (Richtmyer and Morton, 1967, p. 198)

$$(T_s)_\ell = E_\ell(T_s)_{\ell+1} + F_1 , \tag{29}$$

where  $(T_s)_\ell$  is the soil temperature at the  $\ell^{\text{th}}$  grid level from the surface. Expressions for  $E_\ell$  and  $F_\ell$  when  $\ell > 1$  are determined from the finite-difference form of Eq. (16), and Eq. (28) determines  $E_1$  and  $F_1$ . From Eqs. (28) and (29), we obtain

$$E_1 = \left( \frac{K_s}{\Delta z_s} \right) / \left[ 4\epsilon\sigma(T_G^n)^3 + m \left( \frac{P_o}{P_G} \right)^{R/c_p} + \frac{K_s}{\Delta z_s} \right] , \tag{30}$$

and

$$F_1 = \frac{[R_s + \epsilon R_L \downarrow + 3\epsilon\sigma(T_G^n)^4 + m\Theta^n(z_1)]}{[4\epsilon\sigma(T_G^n)^3 + m \left( \frac{P_o}{P_G} \right)^{R/c_p} + \left( \frac{K_s}{\Delta z_s} \right)]} . \tag{31}$$

Numerical integration of Eq. (16) by use of Eq. (29) to Eq. (31) is rapid since no iteration is required.

The incoming direct solar radiation flux to an inclined surface is obtained from Kondratyev (1977):

$$R_s = R_o[A + B \cos \Omega + C \sin \Omega] \tag{32}$$

where

$$A = \cos \alpha \sin \phi \sin \delta + \sin \alpha \cos \Psi_n (\tan \Phi \sin \Phi \sin \delta - \sin \delta \sec \Phi) \quad (33a)$$

$$B = \cos \alpha \cos \Phi \cos \delta + \sin \alpha \cos \Phi \sin \Phi_n \cos \delta , \quad (33b)$$

and

$$C = \sin \alpha \cos \delta \sin \Phi_n . \quad (33c)$$

In the above expressions  $R_o$  is the near surface, direct solar radiation flux;  $\Omega$  is the solar hour angle, positive clockwise from apparent noon;  $\Phi$  is the latitude;  $\delta$  is the declination of the sun;  $\alpha$  is the angle of inclination of the surface relative to the horizontal plane; and  $\Psi_n$  is the azimuth of the projection of the normal to the surface on the horizontal plane, as counted from the plane of the meridian (azimuth is considered positive when counted clockwise). Since the maximum change in the solar declination  $\delta$  in 24 hours is less than 0.5 degrees,  $\delta$  is assumed to be constant during a given day. Spencer (1971, quoted in Paltridge and Platt, 1976, p. 63) provides a formula to compute  $\delta$  in radians,

$$\begin{aligned} \delta = & 0.006918 - 0.399912 \cos \theta_o + 0.070257 \sin \theta_o \\ & - 0.006758 \cos 2\theta_o + 0.000907 \sin 2\theta_o \\ & - 0.002697 \cos 3\theta_o + 0.001480 \sin 3\theta_o , \end{aligned} \quad (34)$$

where the angle  $\theta_o$  in radians is related to the Julian day  $J_d$  by

$$\theta_o = \frac{2\pi(J_d - 1)}{365} . \quad (35)$$

Equation (34) estimates  $\delta$  with a maximum error of 0.0006 radians. Solar hour  $\Omega$  can be obtained if the longitude, clocktime, and the equation of time are known. The equation of time is the difference between the local apparent time and a fixed mean solar time, which is derived from the motion of a celestial equation at a rate equal to the average movement of the sun. The solar hour angle  $\Omega$  is given in radians by

$$\Omega = \frac{\pi(t_s - 12)}{12} , \quad (36)$$

where  $t_s$  is the true solar time (local apparent time) in hours. The true solar time is obtained from

$$t_s = t_{c.t.} + \Delta t_{long} + t_{eq} \quad (37)$$

where  $t_{c.t.}$ ,  $\Delta t_{long}$ , and  $t_{eq}$  are the clocktime, the longitude correction, and the equation of time, respectively. The longitude correction accounts for the difference between the local meridian and a standard meridian, and is positive if the local meridian is east of the standard. The equation of time is provided by Spencer (quoted in Paltridge and Platt, 1976, p. 63) as follows;

$$\begin{aligned} t_{eq} = & \frac{12}{\pi} (0.000075 + 0.001868 \cos \theta_o \\ & - 0.032077 \sin \theta_o - 0.014615 \cos 2\theta_o \\ & - 0.40849 \sin 2\theta_o) \quad , \end{aligned} \quad (38)$$

where  $t_{eq}$  is in hours and  $\theta_o$  is defined by Eq. (35). Equation (38) has a maximum error, compared with values tabulated in the National Almanac, of 35 s in time.

The amount of solar radiation reaching the surface is much less than that at the top of the atmosphere due to many factors, including molecular scattering and absorption by permanent gases such as oxygen, ozone, and carbon dioxide. The effect is parameterized by Atwater and Brown (1974), who modified the original form by Kondratyev (1969) to include the effect of the forward Rayleigh scattering. The expression is

$$\begin{aligned} G = & 0.485 \\ & + 0.515 \left[ 1.041 - 0.16 \left( \frac{0.000949P + 0.051}{\cos Z} \right)^{1/2} \right] \end{aligned} \quad (39)$$

where  $P$  is pressure in  $mb$ . Other important factors that also modify the amount of incoming solar radiation include water vapor, clouds, and airborne particles. Parameterizations for these factors are not included in the present model.

Currently  $R_o$  in Eq. (32) is calculated from

$$R_o = R_{\infty}G , \quad (40)$$

where  $R_{\infty}$  is the incoming radiation flux at the top of the atmosphere and  $G$  is given by Eq. (39).

The zenith angle  $Z$  in Eq. (39) is determined from the following formula

$$\cos Z = \sin \Phi \sin \delta + \cos \Phi \cos \delta \cos \Omega . \quad (41)$$

Finally,  $R_L \downarrow$ , the long-wave incoming radiation at the surface, is computed according to the following formula

$$R_L \downarrow = R_o \downarrow \cos \alpha \quad (42)$$

where  $R_o \downarrow$  is the long-wave incoming radiation normal to horizontal surface and  $\alpha$  is the angle of inclination of a sloped surface given by

$$\alpha = \tan^{-1} \left[ \left( \frac{\partial z_g}{\partial x} \right)^2 + \left( \frac{\partial z_g}{\partial y} \right)^2 \right]^{1/2} . \quad (43)$$

Boundary conditions for  $U, V, \Theta, Q_v, q$ , and  $\ell$  along the upper computational boundary are

$$(U, V) = (U_g, V_g), \quad (44a, b)$$

where  $U_g$  and  $V_g$  are geostrophic wind components defined as

$$(U_g, V_g) = (1/f) \left( \frac{-\partial P}{\partial y} \right), \left( \frac{\partial P}{\partial x} \right) . \quad (45a, b)$$

Potential temperature and the mixing ratio are specified, and turbulence is assumed to vanish along the upper boundary. Soil temperature at 30 cm below the surface is also specified.

The lateral boundary values for  $U, V, \Theta, Q_v, q^2$ , and  $\ell$  are obtained by integrating the corresponding governing Eqs. (2), (3), (10), (11), (12), and (13), except that variations

in the horizontal directions are all neglected. Variables  $U, V, q^2$ , and  $q^2 \ell$  are smoothed at each time step by using the values at four neighboring points, i.e.,

$$\Phi_{i,j} = (1 - \lambda)\Phi_{i,j} + 0.25\lambda(\Phi_{i+1,j} + \Phi_{i-1,j} + \Phi_{i,j-1} + \Phi_{i,j+1}) , \quad (46)$$

where  $\Phi$  represents either  $U, V, q^2$ , or  $q^2 \ell$ , and  $\lambda = 0.5$  is used. A similar expression, but using only three neighboring points, is applied to the values at the lateral boundaries.

For use on a microcomputer, two modifications have been made. First, changes have been made in the code that destroy the effects of terrain slopes at the boundaries. This makes it possible to put the boundaries in very complex terrain without constructing an artificial apron around the area of interest. The second change was to force the first grid vertical cell to be at 4 m aboveground. This change was to ensure that the lowest layer was sufficiently near the ground to generate the appropriate slope flows.

**Initial Values.** An initial wind profile at the southwestern corner of the computational domain is first constructed by assuming a logarithmic variation (initially  $u_* = 0.2$  m/s, and  $z_o = 0.1$  m) from the ground up to the level where the wind speed reaches an ambient value (geostrophic wind). Initial wind profiles at other grid locations are obtained by scaling the southwestern corner winds to satisfy the mass continuity.

The vertical profile of potential temperature is initially assumed to increase linearly with height. Initial potential temperatures are assumed to be uniform in the horizontal directions. Initial values for water vapor are constructed by using the initial potential temperature profiles, pressure at the top of computational domain, and observed relative humidity. The turbulence kinetic energy and length scale are initialized by using the initial wind and temperature profiles and the relationships resulted from the level 2 model. These expressions are already given by Yamada (1975) and are not repeated here.

**Numerical Procedures.** The partial differential Eqs. (2), (3), and (10) to (13) are integrated by using the Alternating Direction Implicit (ADI) method, and a time increment is chosen to satisfy Courant-Friedrich-Lewy criteria. In order to increase the accuracy of finite-difference approximations, mean and turbulence variables are defined at grids that are staggered both in horizontal and vertical directions (see Section IV). Mean winds, temperatures, and water vapor vary greatly with height near the surface. In order



to resolve these variations, nonuniform grid spacings are used in the vertical direction.

### B. RAPTAD (Random Particle Transport And Diffusion.)

A brief description of the RAPTAD model is given here. Locations of particles are computed from

$$x_i(t + \Delta t) = x_i(t) + U_{pi}\Delta t , \quad (47)$$

where

$$U_{pi} = U_i + u_i , \quad (48)$$

$$u_i(t + \Delta t) = au_i(t) + b\sigma_u\zeta + \delta_{i3}(1 - a)t_{Lz}\frac{\partial}{\partial x_i}(\sigma_{u_i}^2) , \quad (49)$$

$$a = \exp(-\Delta t/t_{Lz}) , \quad (50)$$

and

$$b = (1 - a^2)^{1/2} . \quad (51)$$

In the above expressions,  $U_{pi}$  is the particle velocity in  $x_i$  direction,  $U_i$  mean velocity,  $u_i$  turbulence velocity,  $\zeta$  a random number from a Gaussian distribution with zero mean and unit variance,  $t_{Lz}$  the Lagrangian integral time for the velocity  $u_i$ ,  $\sigma_{u_i}$  variance of velocity fluctuation  $u_i$ , and  $\delta_{i3}$  is the Dirac delta. The last term on the right-hand side of Eq. (49) was introduced by Legg and Raupach (1982) in order to correct accumulation of particles in the low energy areas. The mean velocity  $U_i$  and vertical velocity variance  $\sigma_i$  are obtained from the hydrodynamic model results discussed in Section III.A. The Lagrangian time scales,  $t_{Lz} = 20s$ ,  $t_{Lx} = 5000s$ , and  $t_{Ly} = 5000s$ , are used in this study.

In the previous studies (Yamada, 1981 and 1985), the concentration at a given time and location was determined by counting the number of particles in an imaginary sampling volume. The computed concentration level could vary considerably depending on the size of the sampling volume and number of particles used in the computation. For example,

if the sampling volume is very small, the concentration distribution becomes very noisy. On the other hand, if the sampling volume is too large, the concentration distribution will be oversmoothed (Yamada et al., 1987a). Theoretically, the sampling volume problem is eliminated by releasing an infinite number of particles in the computation. Of course, it is impossible in practice, or at least very expensive, to release an infinite number of particles.

A “kernel” density estimator is used in this study where each particle represents a center of a puff. Various functional forms can be assumed to express the concentration distribution in the puff. One of the simplest ways is to assume a Gaussian distribution where variances are determined as the time integration of the velocity variances encountered over the history of the puff. The concentration level at a given time and space is determined as the sum of the concentrations each puff contributes. The kernel method requires no imaginary sampling volumes and produces smooth concentration distribution with a much smaller number of particles than required for the previous particle method (Yamada et al., 1987a).

Concentration  $\chi$  at  $(X, Y, Z)$  is estimated by using the following expression:

$$\begin{aligned} \chi(X, Y, Z) = & \frac{Q\Delta t}{(2\pi)^{3/2}} \sum_{k=1}^N \frac{1}{\sigma_{x_k} \sigma_{y_k} \sigma_{z_k}} \exp\left(-\frac{1}{2} \frac{(x_k - X)^2}{\sigma_{x_k}^2}\right) \\ & \bullet \exp\left(-\frac{1}{2} \frac{(y_k - Y)^2}{\sigma_{y_k}^2}\right) \\ & \bullet \left[ \exp\left(-\frac{1}{2} \frac{(z_k - Z)^2}{\sigma_{z_k}^2}\right) + \exp\left(-\frac{1}{2} \frac{(z_k + Z - 2z_g)^2}{\sigma_{z_k}^2}\right) \right] \end{aligned} \quad (52)$$

where  $(x_k, y_k, z_k)$  is the location of  $k$  th particle;  $\sigma_{x_k}, \sigma_{y_k}$  and  $\sigma_{z_k}$  are standard deviations of a Gaussian distribution; and  $z_g$  is the ground elevation. The variances are estimated based on Taylor’s (1921) homogeneous diffusion theory. For example,  $\sigma_y$  is obtained from

$$\begin{aligned} \sigma_y^2 &= 2\sigma_v^2 \int_0^t \int_0^\zeta R(\zeta) d\zeta dt \\ &= 2\sigma_v^2 t L_y \left( t + t L_y \exp\left(-\frac{t}{t L_y}\right) - t L_y \right), \end{aligned} \quad (53)$$

where a correlation function  $R(\zeta) = \exp\left(\frac{-\zeta}{t_{Ly}}\right)$  is used. Equation (53) is approximated by

$$\sigma_y = \sigma_v t \text{ for } t \leq 2t_{Ly} , \quad (54a)$$

and

$$\sigma_y^2 = 2t_{Ly}\sigma_v^2 t \text{ for } t > 2t_{Ly} . \quad (54b)$$

Although the turbulence field under the study is not homogeneous, we assume the theory can be applicable over a short time period, such as an integration time step (10 sec. in this study). Therefore,

$$\sigma_y(t + \Delta t) = \sigma_y(t) + \sigma_v \Delta t \text{ for } t \leq 2t_{Ly} \quad (55a)$$

and

$$\sigma_y^2(t + \Delta t) = \sigma_y^2(t) + 2t_{Ly}\sigma_v^2 \Delta t \text{ for } t > 2t_{Ly} \quad (55b)$$

are used in this study.

In a similar fashion,

$$\sigma_x(t + \Delta t) = \sigma_x(t) + \sigma_u \Delta t \text{ for } t \leq 2t_{Lx} , \quad (56a)$$

$$\sigma_x^2(t + \Delta t) = \sigma_x^2(t) + 2t_{Lx}\sigma_u^2 \Delta t \text{ for } t > 2t_{Lx} , \quad (56b)$$

$$\sigma_z(t + \Delta t) = \sigma_z(t) + \sigma_w \Delta t \text{ for } t \leq 2t_{Lz} , \quad (57a)$$

and

$$\sigma_z^2(t + \Delta t) = \sigma_z^2(t) + 2t_{Lz}\sigma_w^2 \Delta t \text{ for } t > 2t_{Lz} , \quad (57b)$$

where the standard deviations  $\sigma_u$ ,  $\sigma_v$ , and  $\sigma_w$  at each particle location are obtained by interpolating grid values of a computation grid volume in which a particle is located.

#### IV. FINITE-DIFFERENCE REPRESENTATIONS AND A GRID SYSTEM

The prognostic Eqs. (2), (3), (10), (11), (12), and (13) may be expressed in the following general form:

$$\frac{\partial \phi}{\partial t} = \Delta_x \phi + \Delta_y \phi + \Delta_z \phi - A\phi + F \quad (58)$$

where

$$\Delta_x \phi \equiv \frac{\partial}{\partial x} \left( K_1 \frac{\partial \phi}{\partial x} \right) - U \frac{\partial \phi}{\partial x} , \quad (59a)$$

$$\Delta_y \phi \equiv \frac{\partial}{\partial y} \left( K_2 \frac{\partial \phi}{\partial y} \right) - V \frac{\partial \phi}{\partial y} , \quad (59b)$$

$$\Delta_z \phi \equiv \frac{\partial}{\partial z} \left( K_3 \frac{\partial \phi}{\partial z} \right) - W \frac{\partial \phi}{\partial z} , \quad (59c)$$

and

$$\phi \equiv (U, V, \Theta_t, Q_w, q^2, q^2 \ell) . \quad (60)$$

The coefficient  $K_1$  represents the horizontal eddy viscosity coefficients  $K_x$  or  $K_{xy}$ . Similarly,  $K_2$  represents  $K_y$  or  $K_{xy}$ , and  $K_3$  represents the vertical eddy viscosity coefficients  $K_M$  or  $K_H$ . The fourth and fifth terms on the right-hand side of Eq. (58) represent the variable to which the equation applies and external forcing functions, respectively. Table 1 summarizes  $K_1, K_2, K_3, A$ , and  $F$  for the prognostic equations for  $U, V, \Theta_t, Q_w, q^2$ , and  $q_t^2$ .

The ADI method, developed by Peaceman and Rachford (1955), has second-order accuracy for both space and time derivatives and is unconditionally stable. The ADI scheme has been extensively and successfully applied in the simulation of various one- and two-dimensional fluid dynamics problems (Roache, 1972, p. 95). Generalization of the scheme to a three-dimensional space, however, requires special consideration, as pointed out by Richtmyer and Morton (1967, p. 212); otherwise, the unconditional stability is lost and accuracy drops to  $O(\Delta t) + O[(\Delta x)^2]$ .

The finite-difference version of Eq. (58) may be written according to ADI method as

$$\frac{\phi^* - \phi^n}{\Delta t} = \frac{1}{2} \Delta_x (\phi^* + \phi^n) + \Delta_x \phi^n + \Delta_y \phi^n - A\phi^* + F , \quad (61)$$

$$\frac{\phi^{**} - \phi^n}{\Delta t} = \frac{1}{2} \Delta_z(\phi^* + \phi^n) + \frac{1}{2} \Delta_x(\phi^{**} + \phi^n) + \Delta_y \phi^n - A\phi^* + F, \quad (62)$$

and

$$\begin{aligned} \frac{\phi^{n+1} - \phi^n}{\Delta t} &= \frac{1}{2} \Delta_z(\phi^* + \phi^n) + \frac{1}{2} \Delta_x(\phi^{**} + \phi^n) \\ &+ \frac{1}{2} \Delta_y(\phi^{n+1} + \phi^n) - A\phi^* + F, \end{aligned} \quad (63)$$

where  $\phi^n$  and  $\phi^{n+1}$  are values at  $t = n\Delta t$  and  $(n+1)\Delta t$ , respectively, and  $\Delta t$  is a time increment of integration. The value represented by  $\phi^*$  and  $\phi^{**}$  are the first and second intermediate values necessary to obtain  $\phi^{n+1}$  from  $\phi^n$ . Richtmyer and Morton (1967, p. 213) pointed out that if  $\phi^*$  in the vertical derivative term of Eq. (63) is replaced by the most recent value  $\phi^{**}$ , then the unconditional stability is lost. The amplification factor for the complete cycle given by Eqs. (61) to (63) is shown to be not greater than 1, indicating unconditional stability (Richtmyer and Morton, 1967, p. 213).

TABLE 1. Coefficients  $K_1, K_2, K_3, A$ , and  $F$  in Eq. (58)

$\phi$	$K_1$	$K_2$	$K_3$	$A$	$F$
$U$	$K_x$	$K_{xy}$	$K_M$	0	$f(V - V_g) + g \frac{\bar{H} - z^*}{H} \left(1 - \frac{\langle \theta_v \rangle}{\Theta_v}\right) \frac{\partial z_g}{\partial z}$
$V$	$K_{xy}$	$K_y$	$K_M$	0	$-f(U - U_g) + g \frac{\bar{H} - z^*}{H} \left(1 - \frac{\langle \theta_v \rangle}{\Theta_v}\right) \frac{\partial z_g}{\partial y}$
$\Theta_\ell$	$K_x$	$K_H$	$K_H$	0	$\frac{1}{\rho C_p} \frac{\partial R_N}{\partial z^*}$
$Q_w$	$K_x$	$K_y$	$K_H$	0	0
$\frac{q^2}{2}$	$K_x$	$K_y$	$q\ell\tilde{S}_\ell$	$q/\Lambda_1$	$-\frac{\bar{H}}{H - z_g} \left( \bar{u}w \frac{\partial U}{\partial z^*} + \bar{v}w \frac{\partial V}{\partial z^*} \right) + \beta g \bar{w} \bar{\theta}_v$
$q^2\ell$	$K_x$	$K_y$	$q\ell\tilde{S}_\ell$	$q/\Lambda_1 \times$	$\ell F_1 \frac{\bar{H}}{H - z_g} \left( -\bar{u}w \frac{\partial U}{\partial z^*} - \bar{v}w \frac{\partial V}{\partial z^*} \right) + \beta g \bar{w} \bar{\theta}_v$
					$\left[ 1 + F_2 \left( \frac{\ell}{kz} \right)^2 \right]$

Equations (62) and (63) may be simplified by subtracting Eq. (61) from Eq. (62) and subtracting Eq. (62) from Eq. (63), respectively. The resulting equations are

$$\frac{\phi^{**} - \phi^*}{\Delta t} = \frac{1}{2} \Delta_x(\phi^{**} - \phi^n) \quad (64)$$

and

$$\frac{\phi^{n+1} - \phi^{**}}{\Delta t} = \frac{1}{2} \Delta_y (\phi^{n+1} - \phi^n) . \quad (65)$$

Equations (61), (64), and (65) may be rewritten as

$$\left(1 + A\Delta t - \frac{\Delta t}{2} \Delta_z\right) \phi^* = \phi^n + \Delta t \left\{ \frac{1}{2} \Delta_z \phi^n + \Delta_x \phi^n + \Delta_y \phi^n + F \right\} \quad (66)$$

$$\left(1 - \frac{\Delta t}{2} \Delta_x\right) \phi^{**} = \phi^* - \frac{\Delta t}{2} \Delta_x \phi^n , \quad (67)$$

and

$$\left(1 - \frac{\Delta t}{2} \Delta_y\right) \phi^{n+1} = \phi^{**} - \frac{\Delta t}{2} \Delta_y \phi^n . \quad (68)$$

Equations (66) and (68) may be further transformed to the general form

$$-A_\ell \phi_{\ell-1} + B_\ell \phi_\ell - C_\ell \phi_{\ell+1} = D_\ell , \quad (69)$$

where  $\ell = i, j, k$  represents the  $i, j$ , and  $k$  th grid points in the  $x, y$ , and  $z$  directions, respectively. The space derivatives  $\Delta_x \phi, \Delta_y \phi$ , and  $\Delta_z \phi$  are approximated by centered finite differences. Coefficients  $A_\ell, B_\ell, C_\ell$ , and  $D_\ell$  may be identified by comparing term by term the expanded forms of Eqs. (66) to (68) with those of Eq. (69). The results are given in Table 2.

TABLE 2. Coefficients  $A_\ell, B_\ell, C_\ell$ , and  $D_\ell$  for Eq. (69). The coefficients  $a_i, b_j$ , and  $c_k$  are  $dX/dx, dY/dy$ , and  $dZ/dz$ , respectively, where  $(X, Y, Z)$  are grid coordinates, whose increments are one.

---


$$\begin{aligned} A_k & (c_k \Delta t / 2) \left\{ \frac{W_k^n}{2} + (cK_3)_{k-1/2} \right\} \\ C_k & (c_k \Delta t / 2) \left\{ \frac{-W_k^n}{2} + (cK_3)_{k+1/2} \right\} \\ B_k & 1 + A_k + C_k + A\Delta t \\ D_k & \phi^n + \Delta t \left\{ \frac{1}{2} \Delta_z \phi^n + \Delta_x \phi^n + \Delta_y \phi^n + F \right\} \end{aligned}$$


---

$$A_i \quad (a_i \Delta t / 2) \left\{ \frac{U_i^n}{2} + (aK_1)_i - 1/2 \right\}$$

$$\begin{aligned}
C_i & (a_i \Delta t / 2) \left\{ \frac{-U_i^n}{2} + (aK_1)_i - 1/2 \right\} \\
B_i & 1 + A_i + C_i \\
D_i & \phi_i^* - (\Delta t / 2) \Delta_z \phi^n
\end{aligned}$$


---

$$\begin{aligned}
A_j & (b_j \Delta t / 2) \left\{ \frac{V_j^n}{2} + (bK_2)_{j-1/2} \right\} \\
C_j & (b_j \Delta t / 2) \left\{ \frac{-V_j^n}{2} + (bK_2)_{j+1/2} \right\} \\
B_j & 1 + A_j + C_j \\
D_j & \phi_j^{**} - (\Delta t / 2) \Delta_y \phi^n
\end{aligned}$$


---

Equation (69) may be expressed in the general form  $\mathcal{T}\phi = \mathcal{S}$ , where  $\mathcal{T}$  is a tridiagonal matrix whose elements are given by  $A_\ell, B_\ell$ , and  $C_\ell$ , and  $\mathcal{S}$  is a column vector whose elements are given by  $D_\ell$ . Solutions for Eq. (69), whose coefficient matrix is tridiagonal, are obtained by a direct elimination method (Richtmyer and Morton, 1967, p. 200).

Accuracy of a finite-difference approximation is enhanced if the grid is defined in such a manner that the variables vary linearly with the coordinates. For example, wind, temperature, and water vapor are known to vary approximately logarithmically with height in the surface layer if corrections for atmospheric stability are minor. Those variables, however, vary much more slowly with height in the layers away from the surface. Thus, vertical grids are spaced according to a log-plus-linear relation

$$Z = c_1 z + c_2 \ln[(Z + c_3)/c_3] , \quad (70)$$

where  $Z$  is a transformed vertical coordinate (representing the grid level) whose increment is one and  $c_1, c_2$ , and  $c_3$  are constants to be determined, depending on the problem to be solved.

In order to increase the accuracy of finite-difference approximations and to suppress computational noise whose wave length is  $2\Delta$ , where  $\Delta$  is a grid increment, mean and turbulence variables are defined on a staggered grid. Figure 15 shows relative locations of variables in a grid volume:  $U$  and  $V$  in Fig. 15a;  $\Theta_\ell$  and  $Q_w$  in Fig. 15b; and  $q^2$  and  $q_\ell^2$  in Fig. 15c.

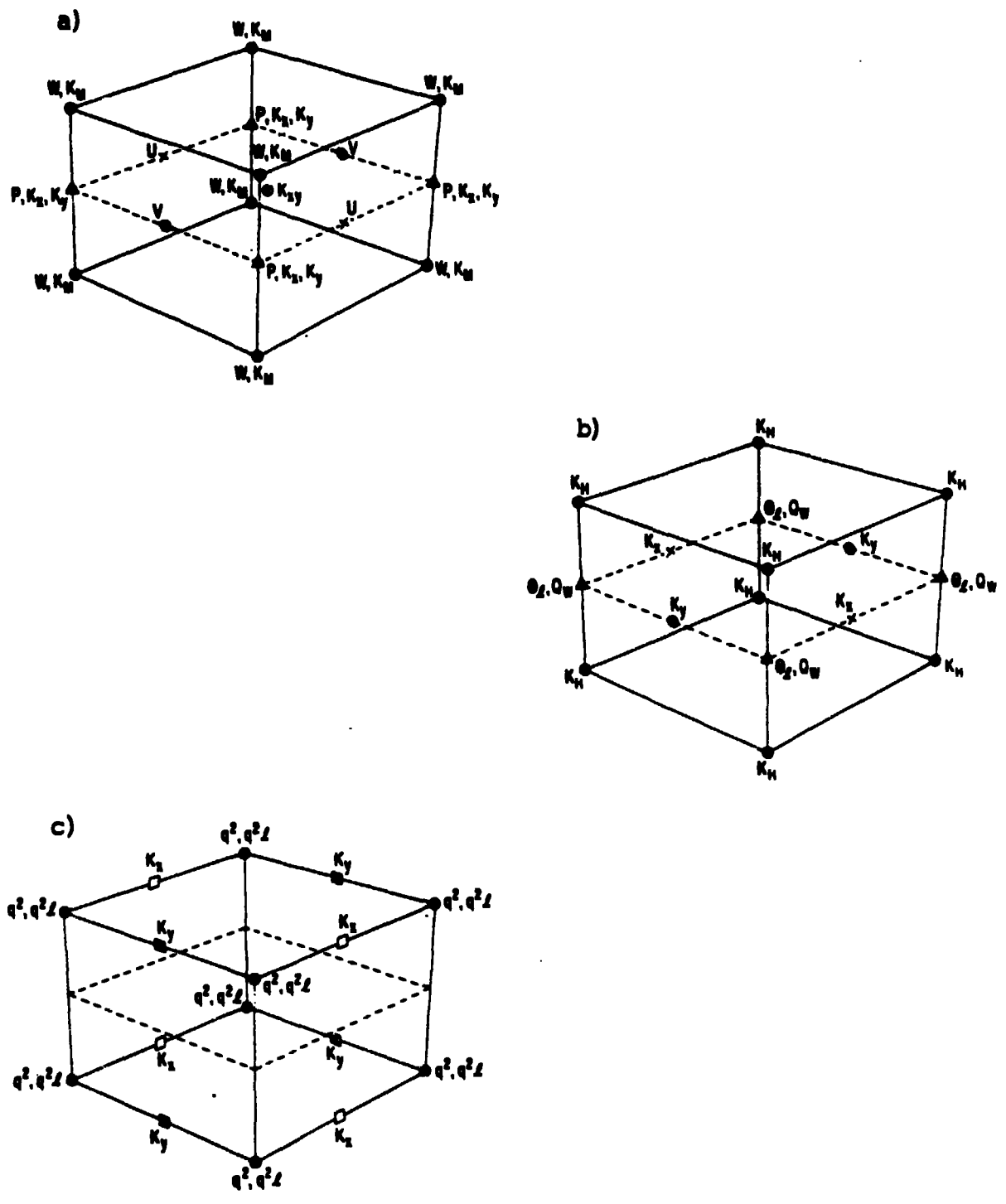


Fig. 15. Relative locations of mean and turbulence variables in the computational grid: a)  $U$  and  $V$ , b)  $\Theta_L$  and  $Q_w$ , and c)  $q^2$ , and  $q^2_L$ .



**Boundary Conditions.** As shown by Mellor (1973), our model simulated the surface layer data reported by Businger et al. (1971) quite well. A rather coarse vertical grid spacing is necessary for three-dimensional modeling due to limitations of storage and time. Thus, in order to increase accuracy, empirical surface-layer parameterization is used for the first and second grid levels above the ground. Wind, temperature, and water vapor profiles in the surface layer may be approximated by the following formulas:

$$\frac{|\underline{V}(z)|}{u_*} = \frac{1}{k} [\ln\{(z + z_o)/z_o\} - \psi_m(\zeta)] , \quad (71)$$

$$\frac{\Theta_\ell(z) - \Theta_\ell(0)}{T_*} = \frac{P_r}{k} [\ln\{(z + z_{ot})/z_{ot}\} - \psi_h(\zeta)] , \quad (72)$$

$$\frac{Q_w(z) - Q_w(0)}{Q_*} = \frac{S_c}{k} [\ln\{(z + z_{ov})/z_{ov}\} - \psi_v(\zeta)] , \quad (73)$$

$$q^2(z) = B_1^{2/3} u_*^2 (\phi_m - \zeta)^{2/3} , \quad (74)$$

and

$$q^2 \ell(z) = kzq^2(z) . \quad (75)$$

In the above equations,  $\underline{V}(z)$ ,  $\Theta_\ell(z)$ , and  $Q_w(z)$  are the abbreviations for  $\underline{V}(x, y, z, t)$ ,  $\Theta_\ell(x, y, z, t)$ , and  $Q_w(x, y, z, t)$ , respectively, and  $|\underline{V}|$  is the horizontal wind speed  $(U^2 + V^2)^{1/2}$ . Terms  $u_*$ ,  $T_*$ , and  $Q_*$ , defined as  $u_* \equiv \sqrt{\tau/\rho}$ ,  $T_* \equiv H/\rho c_p u_*$ , and  $Q_* \equiv E/\rho_*$ , are friction velocity and scales for temperature and water vapor, respectively. Terms  $\rho$ ,  $H$ , and  $E$  are surface stress, total sensible heat, and rate of evaporation, respectively; total sensible heat being defined as  $H = \overline{w\theta_v} = (1 + 0.61Q_w)\overline{w\theta} + 0.61\overline{wq_w}$ . The parameter  $\zeta$  is a nondimensional height  $z/L$ , where  $L$  is the Obukhov length -  $u_*^3/k\beta gH$ ;  $k$  is the von Karman constant;  $z_o$ ,  $z_{ot}$ , and  $z_{ov}$  are roughness lengths for wind, temperature, and water vapor, respectively; and  $P_r$  and  $S_c$  are the turbulence Prandtl and Schmidt numbers, respectively. Terms  $\psi_m$ ,  $\psi_h$ , and  $\psi_v$  (Panofsky, 1963) are correction terms for the atmospheric stability, and their functional forms are given by

$$\psi_m(\zeta) = \int_0^\zeta \left( \frac{1 - \phi_m(\zeta')}{\zeta'} \right) d\zeta' , \quad (76)$$

$$\psi_h(\zeta) = \int_0^\zeta \left( \frac{1 - \phi_h(\zeta')}{\zeta'} \right) d\zeta' , \quad (77)$$

and

$$\psi_v(\zeta) = \int_0^\zeta \left( \frac{1 - \phi_v(\zeta')}{\zeta'} \right) d\zeta' , \quad (78)$$

where  $\phi_m, \phi_h, \phi_v$  are nondimensional wind, temperature, and water vapor gradients, respectively. The following formulations (Businger, 1966; Dyer and Hicks, 1970) are used for  $\phi_m, \phi_h$ , and  $\phi_v$  under unstable conditions,

$$\phi_m(\zeta) \equiv \frac{kz}{u_*} \frac{\partial U}{\partial z} = (1 - 15\zeta)^{-1/4} , \quad (79)$$

$$\phi_h(\zeta) \equiv \frac{kz}{T_*} \frac{\partial \Theta_t}{\partial z} = (1 - 15\zeta)^{-1/2} , \quad (80)$$

and

$$\phi_v(\zeta) \equiv \frac{kz}{Q_*} \frac{\partial Q_w}{\partial z} = (1 - 15\zeta)^{-1/2} . \quad (81)$$

For stable conditions,

$$\phi_m(\zeta) = \phi_h(\zeta) = \phi_v(\zeta) = 1 + 5\zeta . \quad (82a, b, c)$$

The roughness lengths  $z_o, z_{ot}$ , and  $z_{ov}$  are specified over land and are computed over water according to the following formulas:

$$z_o = \frac{\gamma u_*^2}{g} \quad (83a)$$

$$z_{ot} = \frac{\alpha}{ku_*} \quad (83b)$$

and

$$z_{ov} = \frac{\eta}{ku_*} \quad (83c)$$

(see Sverdrup, 1951; Sheppard, 1958), where  $\gamma$  is a constant whose numerical value varies from 0.008 to 0.032 for water surfaces varying from a lake to a rough ocean and  $\alpha$  and  $\eta$  are the molecular diffusivities for heat and water vapor, respectively. Integrations of Eqs. (76) to (78) may be performed easily (Paulson, 1970). The scales  $u_*, T_*$ , and  $Q_*$  may be

obtained by solving iteratively Eqs. (71) to (81) under unstable conditions. Solutions may be obtained without iteration for stable conditions over land. Iterations are required over the water, however, since the roughness heights are also functions of  $u_*$ , as seen in Eqs. (82a-c.)

Solutions of Eq. (69) may be obtained using the boundary conditions discussed above and following the algorithms described in Richtmyer and Morton (1967, p. 200). Solutions are assumed to be given by a relation

$$\phi_\ell = E_\ell \phi_{\ell+1} + F_\ell \quad (84)$$

where  $E_\ell$  and  $F_\ell$  are determined from

$$E_\ell = \frac{C_\ell}{B_\ell - A_\ell E_{\ell-1}}, \ell > 1, \quad (85a)$$

$$F_\ell = \frac{D_\ell + A_\ell F_{\ell-1}}{B_\ell - A_\ell E_{\ell-1}}, \ell > 1, \quad (85b)$$

where coefficients  $A_\ell, B_\ell, C_\ell,$  and  $D_\ell$  are given in Table 2. The first values  $E_1$  and  $F_1$  may be determined from the surface boundary conditions given by Eqs. (71) and (75). For example, for  $\tilde{V}$  and  $\Theta_\ell$ ,

$$\tilde{V}(z_1) = \frac{\ln\{(z_1 + z_o)/z_o\} - \psi_m(\zeta_1)}{\ln\{(z_2 + z_o)/z_o\} - \psi_m(\zeta_2)} \tilde{V}(z_2) \quad (86)$$

and

$$\begin{aligned} \Theta_\ell(z_1) &= \frac{\ln\{(z_1 + z_{ot})/z_{ot}\} - \psi_h(\zeta_1)}{\ln\{(z_2 + z_{ot})/z_{ot}\} - \psi_h(\zeta_2)} \Theta_\ell(z_2) \\ &\div \left[ 1 - \frac{\ln\{(z_1 + z_{ot})/z_{ot}\} - \psi_h(\zeta_1)}{\ln\{(z_2 + z_{ot})/z_{ot}\} - \psi_h(\zeta_2)} \right] \Theta_\ell(0) \end{aligned} \quad (87)$$

where  $z_1$  and  $z_2$  are the first and second grid levels above the surface, respectively. Comparison between Eq. (84) and Eq. (86), where  $\phi = \tilde{V}$ , yields

$$E_1 = \frac{\ln\{(z_1 + z_o)/z_o\} - \psi_m(\zeta_1)}{\ln\{(z_2 + z_{ot})/z_{ot}\} - \psi_h(\zeta_2)} \quad (88a)$$

and

$$F_1 = 0 \quad . \quad (88b)$$

Similarly, comparison between Eq. (84) and Eq. (87), where  $d = R$ , yields

$$E_1 = \frac{\ell n\{(z_1 + z_{ot})/z_{ot}\} - \psi_h(\zeta_1)}{\ell n\{(z_2 + z_{ot})/z_{ot}\} - \psi_h(\zeta_2)} \quad (89a)$$

and

$$F_1 = (1 - E_1)\Theta_\ell(0) \quad . \quad (89b)$$

Similar expressions as in Eqs. (89a) and (89b) are valid for  $Q_w$ , except that  $z_{ot}$  is replaced by  $z_{ov}$ . When boundary values are specified, as in the case of  $q^2$  and  $q^2\ell$  [Eqs. (74) and (75)],  $E_1$  and  $F_1$  are easily obtained. By comparing Eq. (84) with Eq. (74) we obtain for  $q^2$ .

$$E_1 = 0 \quad (90a)$$

and

$$F_1 = B_1^{2/3} u_*^2 (\phi_m - z_1/L)^{2/3} \quad . \quad (90b)$$

Similarly, by comparing Eq. (84) with Eq. (75) we obtain for  $q^2\ell$

$$E_1 = 0 \quad (91a)$$

and

$$F_1 = k z_1 q^2(z_1) \quad . \quad (91b)$$

Once  $E_1$  and  $F_1$  are determined as described above,  $E_\ell$  and  $F_\ell$  ( $\ell > 1$ ) may be computed according to Eqs. (85a) and (85b), respectively. Then solutions may be computed from Eq. (84), provided the value at the upper boundary is determined from upper boundary conditions as follows. The boundary conditions at the top are assumed to be

$$U = U_g(\bar{H}); V = V_g(\bar{H}) , \quad (92a, b)$$

$$\Theta = \Theta(\bar{H}) , \quad (93)$$

$$Q_w = Q_w(\bar{H}) = 0 , \quad (94)$$

$$q^2 = 0 , \quad (95)$$

and

$$q^2 \ell = 0 . \quad (96)$$

At lateral boundaries, wind, temperature, water vapor,  $q^2$ , and  $q^2 \ell$  are computed from the one-dimensional versions of the corresponding Eqs. (2), (3), (10), (11), (12), and (13).

#### ACKNOWLEDGEMENTS

The authors are grateful to Dr. W. Clements for reviewing the manuscript, C. Thaeler for running the code on various machines, and K. Coen for typing the manuscript. The work is supported by the U. S. Army Nuclear and Chemical Agency. It was performed under the auspices of the U. S. Department of Energy at Los Alamos National Laboratory

## REFERENCES

- Atwater, M. A. and P.S. Brown, Jr., 1974: "Numerical Calculation of the Latitudinal Variation of Solar Radiation for an Atmosphere of Varying Opacity," *J. Appl. Meteor.*, **13**, 289-297.
- Briggs, M. S., G. L. Mellor and T. Yamada, "A Second Moment Turbulence Model Applied to Fully Separated Flows," in *Project Squid Workshop on Turbulence in Internal Flows: Turbomachinery and Other Applications*, S.N.B. Murthy (Ed.) Hemisphere Publishing Corporation, Washington, 1977, 249-281.
- Burk, S. D., 1977, "The Moist Boundary Layer with a Higher Order Turbulence Closure Model," *J. Atmos. Sci.*, **34**, 629-638.
- Businger, J. A., 1966, "Transfer of Momentum and Heat in the Planetary Boundary Layer," Proc. Symp. on the Arctic Heat Budget and Atmospheric Circulation, J. P. Feltcher, Ed., Jan. 31-Feb.4, Lake Arrowhead, California, The Rand Corp., Santa Monica, Calif., Memorandum RM-5233-NSF.
- \_\_\_\_\_, J. C. Wyngaard, Y. Izumi, and E. F. Bradley, 1971, "Flux Profile Relationships in the Atmospheric Surface Layer," *J. Atmos. Sci.*, **28**, 181-189.
- Dobosy, R., 1979, "Dispersion of Atmospheric Pollutants in Flow Over the Shoreline of a Large Body of Water," *J. Appl. Meteor.*, **18**, 117-132.
- Dyer, A. J. and B. B. Hicks, 1970, "Flux-Gradient Relationships in the Constant Flux Layer," *Quart. J. Roy. Meteor. Soc.*, **96**, 715-721.
- Garratt, J. R. and B. B. Hicks, 1973, "Momentum, Heat and Water Vapour Transfer To and From Natural and Artificial Surfaces," *Quart. J. Roy. Met. Soc.*, **99**, 680-687.
- Freeman, B. E., 1977, "Tensor Diffusivity of a Trace Constituent in a Stratified Boundary Layer," *J. Atmos. Sci.*, **34**, 124-136.
- Kao, C.-Y. J., and T. Yamada, 1987, "User of the CAPTEX Data for Evaluations of a Long-Range Transport Numerical Model with a Four-Dimensional Data Assimilation Technique," *Monthly Weather Review* (in press).
- Kondrat'yev, K. Ya., 1969, *Radiation in the Atmosphere*, Academic Press, New York.
- \_\_\_\_\_. 1977, "Radiation Regime of Inclined Surfaces," WMO, Technical Note No. 15, Secretariat of the World Meteorological Organization, Geneva, Switzerland, 82 pp.

- Legg, R. J. and M. F. Raupach, 1982, "Markov-Chain Simulation of Particle Dispersion in Inhomogeneous Flows: The Mean Drift Velocity Induced by a Gradient in Eulerian Velocity Variance," *Boundary-Layer Met.*, **24**, 3-13.
- Mellor, G. L., 1973, "Analytic Predictions of the Properties of Stratified Planetary Surface Layers," *J. Atmos. Sci.*, **30**, 1061-1069.
- Mellor, G. L. and T. Yamada, "A Hierarchy of Turbulence-Closure Models for Planetary Boundary Layers," *J. Atmos. Sci.*, **31**, 1791-1806. Corrigendum, *J. Atmos. Sci.*, **34**, 1482.
- Mellor, G. L. and P. A. Durbin, 1975, "The Structure and Dynamics of the Ocean Surface Mixed Layer," *J. Geophys. Ocean.*, **5**, 718.
- Mellor G. L. and T. Yamada, 1982, "Development of a Turbulence Closure Model for Geophysical Fluid Problems," *Rev. Geophys. Space Phys.*, **20**, 851-875.
- Miyakoda, K. and J. Sirutis, 1977, "Comparative Integrations of Global Models with Various Parameterized Processes of Subgrid Scale Vertical Transports: Descriptions of the Parameterization," *Beitr. Phys. Atmos.*, **50**, 445-487.
- Paltridge, G. W. and C. M. R. Platt, 1976, "Radiative Processes in Meteorology and Climatology," Elsevier Scientific Publishing Company, New York.
- Panofsky, H. A., 1963, "Determination of Stress from Wind and Temperature Measurements," *Q. J. R. Meteorol. Soc.*, **23**, 495-502.
- Paulson, Ca. A., 1970, "The Mathematical Representation of Wind Speed and Temperature Profiles in the Unstable Atmospheric Surface Layer," *J. Appl. Meteorol.*, **9**, 857-861.
- Peaceman, D. W. and H. H. Rachford, Jr., 1955, "The Numerical Solution of Parabolic and Elliptic Differential Equations," *SIAM J. Appl. Math.*, **3**, 28-41.
- Richtmyer, R. D. and K. W. Morton, 1967, "Difference Methods for Initial-Value Problems," Second Ed., *Interscience Publishers*. J. Wiley and Sons, New York, 405 pp.
- Roache, P. J., 1972, *Computational Fluid Dynamics*, Hermosa Publishers, Albuquerque, New Mexico, 434 pp.

- Sasamori, T., 1968, "The Radiative Cooling Calculation for Application to General Circulation Experiments," *J. Appl. Meteor.* **7**, 721-729.
- Shaw, R. H., 1977, "Secondary Wind Speed Maxima Inside Plant Canopies," *J. Appl. Meteor.*, **16**, 514-521.
- Sheppard, P. A., 1958. "Transfer Across the Earth's Surface and Through the Air Above," *Q. J. R. Meteorol. Soc.*, **84**, 205-224.
- Sun, W. Y. and Y. Ogura, 1979, "Boundary-Layer Forcing as a Possible Trigger to a Squall-Line Formation," *J. Atmos. Sci.*, **36**, 235-254.
- Sverdrup, H. U., 1951, "Evaporation from the Oceans," *Compendium of Meteorology*, Waverly Press, Baltimore, 1071-1081.
- Taylor, G. I., 1921, "Diffusion by Continuous Movements," *Proceedings of the London Mathematical Society*, Ser. 2, **20**, 196-211.
- Yamada, T., 1975, "The Critical Richardson Number and the Ratio of the Eddy Transport Coefficients Obtained From a Turbulence Closure Model," *J. Atmos. Sci.*, **32**, 926-933 (May 1975).
- Yamada, T., 1977, "A Numerical Simulation of Pollutant Dispersion in a Horizontally-Homogeneous Atmospheric Boundary Layer," *Atmos. Environ.*, **11**, 1015-1024.
- Yamada, T., 1979, "An Application of a Three-Dimensional Simplified Second-Moment Closure Number Model to Study Atmospheric Effects of a Large Cooling-Pond," *J. Atmos. Environ.*, **13**, 693-704.
- Yamada, T., 1981. "A Numerical Simulation of Nocturnal Drainage Flow," *J. Meteor. Soc. Japan*, **59**, 108-122.
- Yamada, T., 1982, "A Numerical Model Study of Turbulent Airflow In and Above a Forest Canopy," *J. Meteor. Soc. Japan*, **60**, 439-454.
- Yamada, T., 1983, "Simulations of Nocturnal Drainage Flows by a  $q^2$  Turbulence Closure Model," *J. Atmos. Sci.*, **40**, 91-106.
- Yamada, T., 1985, "Numerical Simulations of the Night 2 Data of the 1980 ASCOT Experiments in the California Geysers Area," *Arch. Met. Geoph.*, Ser. **A34**, 223-247.
- Yamada, T. and G. L. Mellor, 1975, "A Simulation of the Wangara Atmospheric Boundary Layer Data," *J. Atmos. Sci.*, **32**, 2309-2329.



- Yamada, T. and G. L. Mellor, 1979, "A Numerical Simulation of the BOMEX Data Using a Turbulence Closure Model Coupled with Ensemble Cloud Relations," *Quart. J. R. Meteorol. Soc.*, **105**, 915-944.
- Yamada, T. and C.-Y. J. Kao. 1986, "A Modeling Study on the Fair Weather Marine Boundary Layer of the GATE," *Journal of Atmospheric Sciences*, **43**, 3186-3199.
- Yamada, T. and S. Bunker, 1988, "Development of a Nested Grid, Second-Moment Turbulence-Closure Model and an Application to the 1982 ASCOT Brush Creek Data Simulation," *Journal of Atmospheric Sciences*, **27**, 562-578.
- Yamada, T., and S. Bunker, 1989: "A Numerical Model Study of Nocturnal Drainage Flows with Strong Wind and Temperature Gradients," *Journal of Applied Meteorology*, **28**, 545-554.
- Yamada, T., S. Bunker, and E. Niccum, 1987a, "Simulations of the ASCOT Brush Creek Data by a Nested-Grid, Second-Moment Turbulence-Closure Model and a Kernel Concentration Estimator," *Proceedings of the Fourth Conference on Mountain Meteorology*, Seattle, WA, Aug. 25-28, 1987, p. 175-179.
- Yamada, T., C.-Y. J. Kao, and S. Bunker, 1987b, "Air Flow and Air Quality Simulations Over the Western Intermountainous Region with a Four-Dimensional Data Assimilation Technique," *Journal of Atmospheric Environment*, **23**, 539-554.

